2022 PICES meeting (09.27.2022)

UC San Diego | SCRIPPS INSTITUTION OF OCEANOGRAPHY

Attribution and predictability of climate-driven variability in global ocean color

Hyung-Gyu Lim

Atmospheric and Oceanic Sciences (AOS) Program, Princeton University (project affiliation)

Scripps Institution of Oceanography, UC San Diego, CA, USA (present affiliation)

With contribution from

NOAA-GFDL: John Dunne, Charlie Stock, KIOST: Minho Kwon

Chlorophyll seasonal cycle

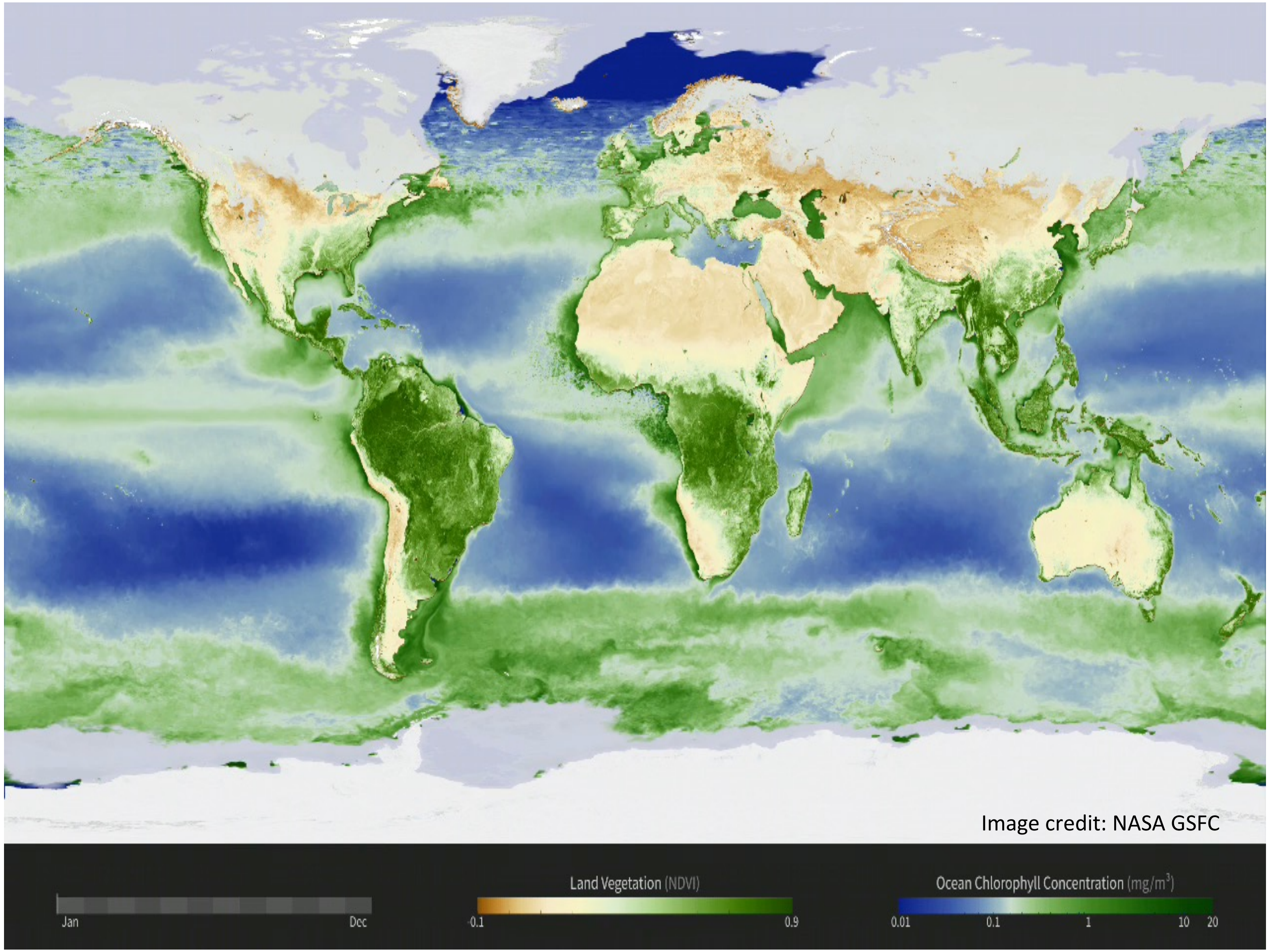

- Optical proxy of marine phytoplankton biomass
- Basis of marine food web resources
- primary production, carbon uptake and carbon export into ocean
- Controlling absorption coefficients of incoming shortwave in ocean layer (Manizza et al. 2005)
- air-sea-bio feedback in Pacific, Indian, Arctic Oceans in GCMs (Anderson et al. 2009; Park et al. 2013;2014;2015; Kim et al. 2015; Kang et al. 2017; Lim et al. 2018;2019;2021)

Chlorophyll timeseries in Satellite era

- Chlorophyll and NPP are decreasing [Behrenfeld et al 2006 Nature]

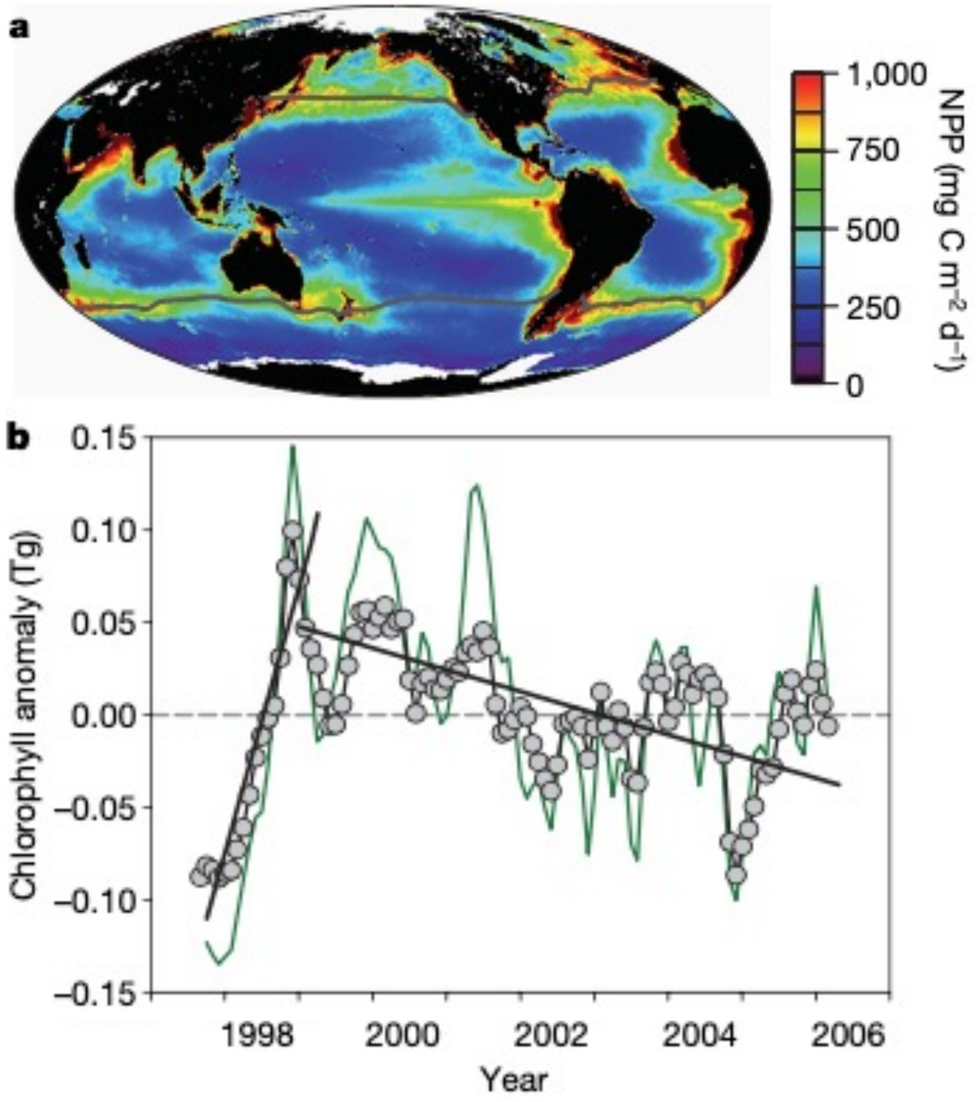

- Oligotrophic region (<0.07mg/m^3) are expanding [Polovina et al. 2008]

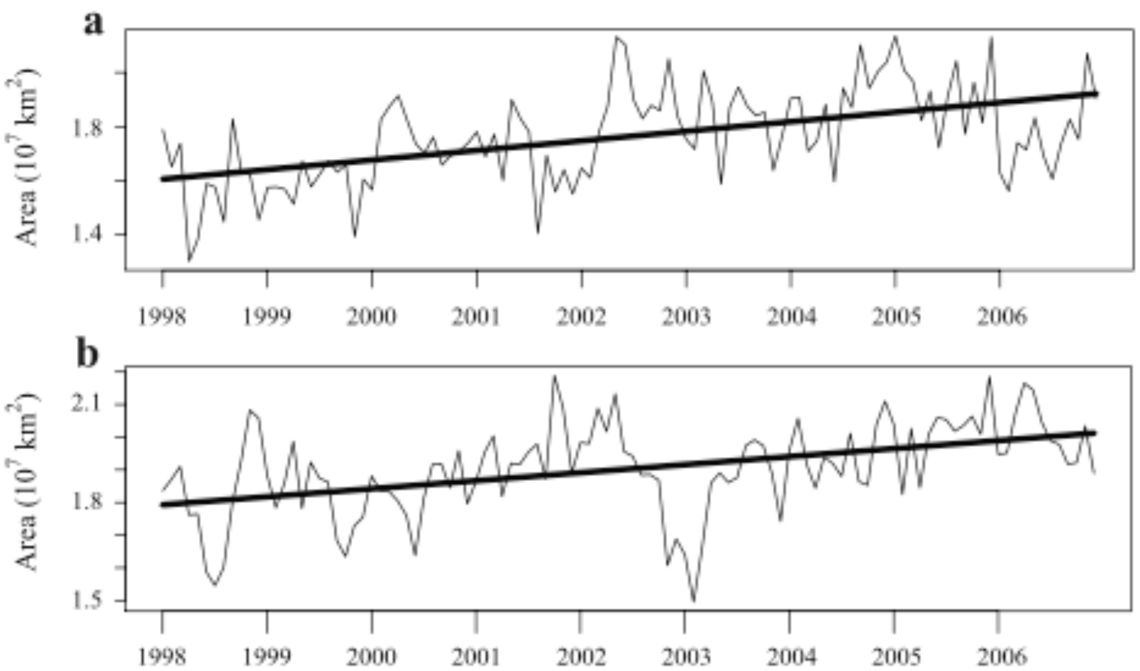

✓ Decreasing CHL trend in addition to events in interannual timescale

Motivation

- To provide the statistical model of SST climate modes (ERSSTv5) related chlorophyll variability using continuous 24-yr satellite ocean color (**GlobColour-GSM**, AVM, ESA-OC-CCI-v5.0) from Sep 1997 to Dec 2021

➢ Ultimate goals are a combination of improved physical prediction for general climate studies and marine ecosystem prediction for living marine resource management

CHL climatology

- ✓ Distributions
  - ➢ High CHL in tropics
  - ➢ Low CHL in subtropics

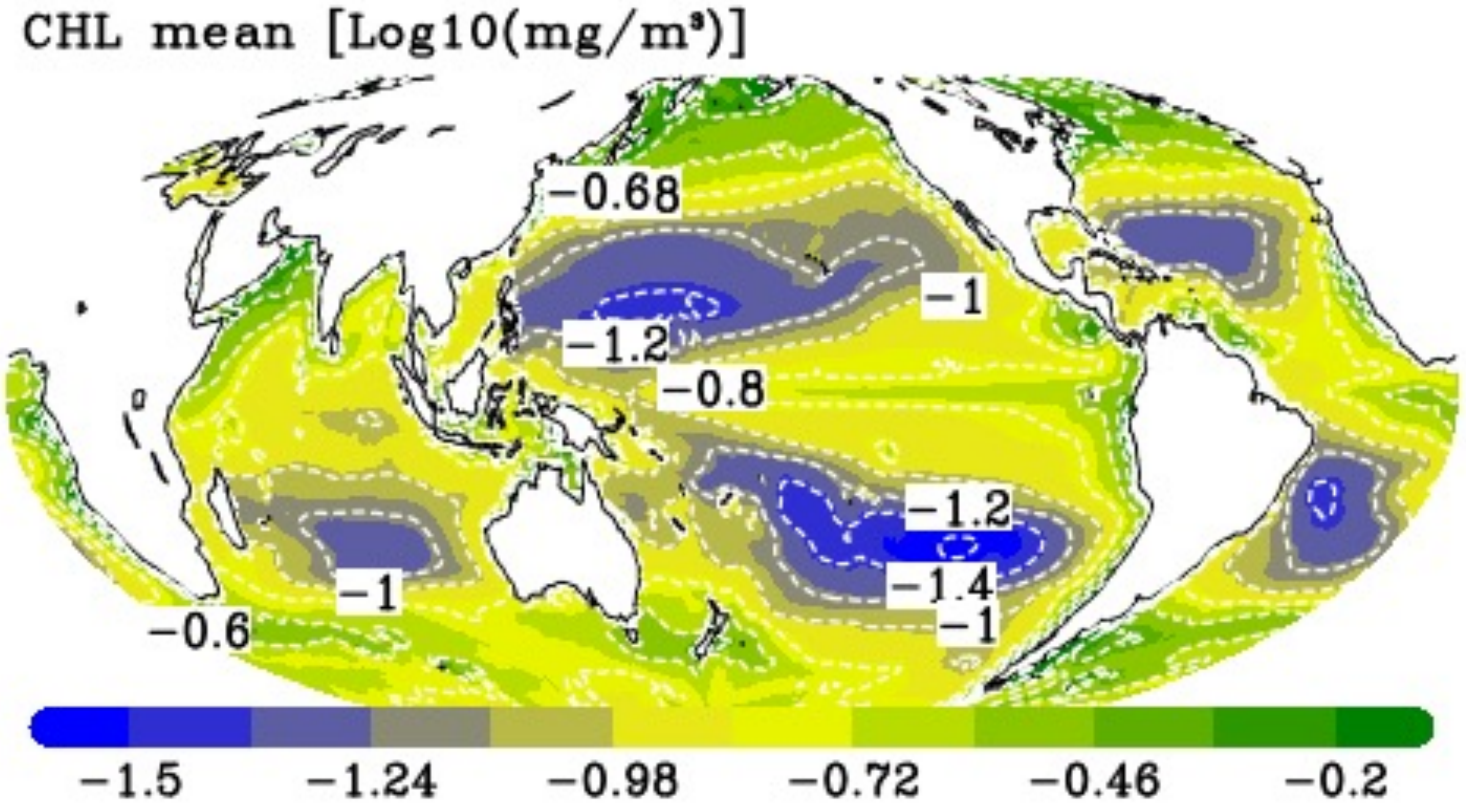

*ESA-CCI-v4.2 sep1997~Apr2020

Total CHL variance (seasonal cycle + interannual variability)

- ✓ Define the major target on CHL variation
  - ➢ High CHL concentration region have high TCV
  - ➢ Oligotrophic region have low TCV

*TCV=$1/N\Sigma(\mathrm{CHL} - \overline{\mathrm{CHL}_{annual}})^2$

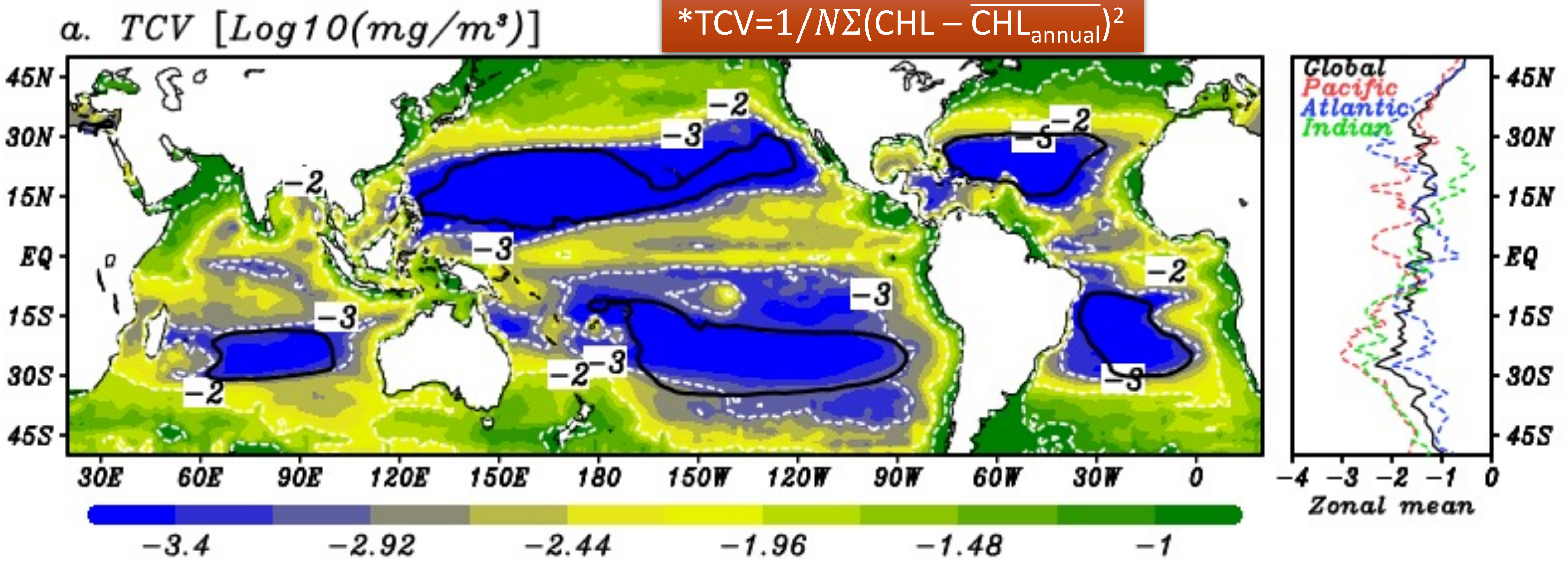

Seasonal cycle contribution on TCV

- Seasonal cycle contributes over 60% in midlatitude (~30°)

Global
Pacific
Atlantic
Indian

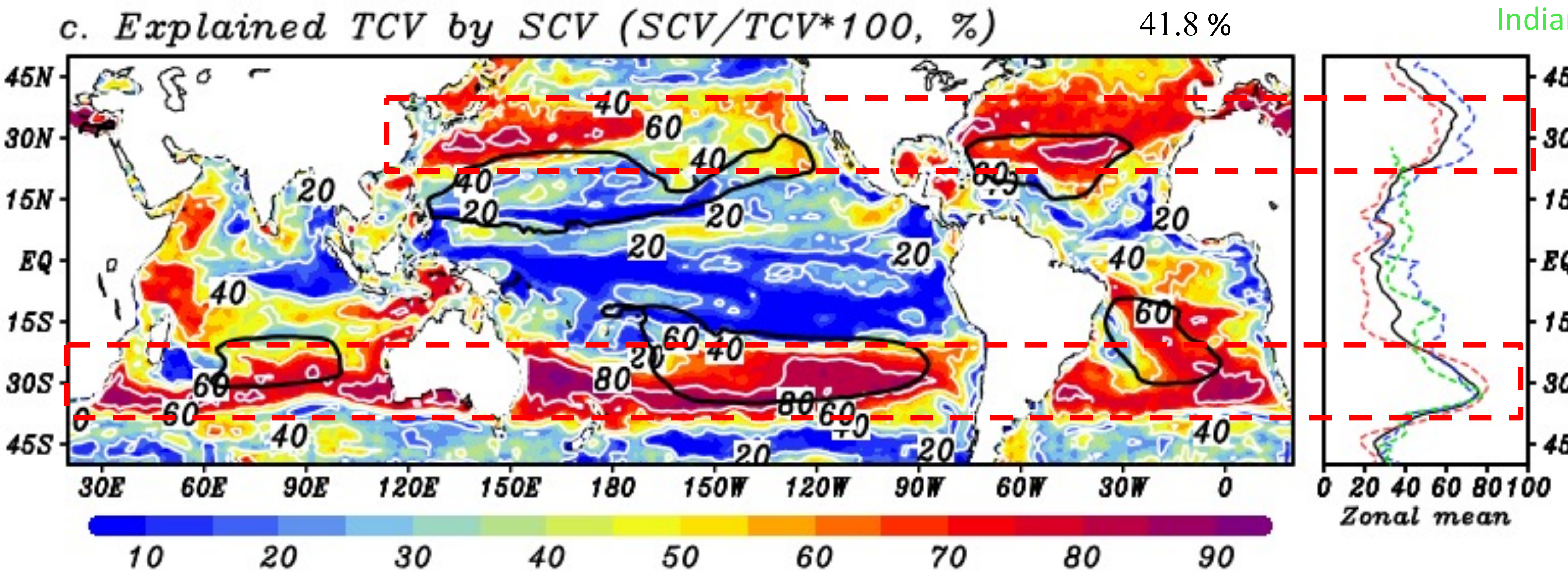

✓ Explained TCV = Var(CHL_SC)/TCV*100

CHL_SC: Reconstructed CHL via Seasonal cycle of CHL only

Seasonal cycle contribution on TCV

- Seasonal cycle contributes over 60% in midlatitude (~30^{o})

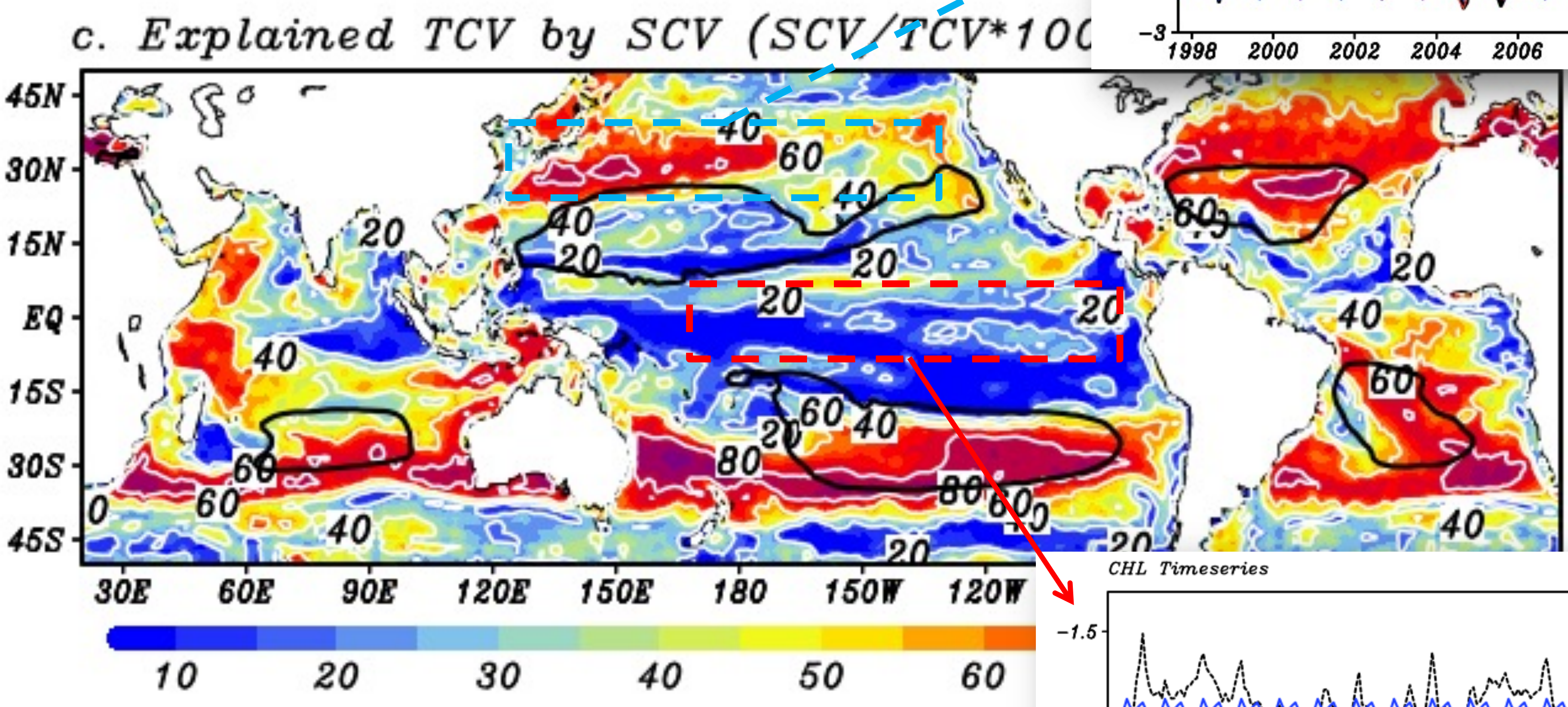

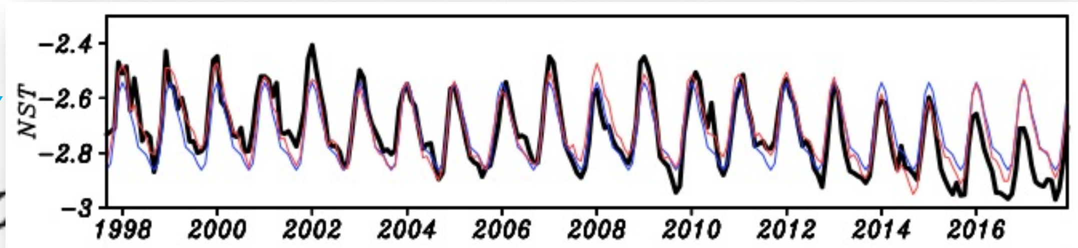

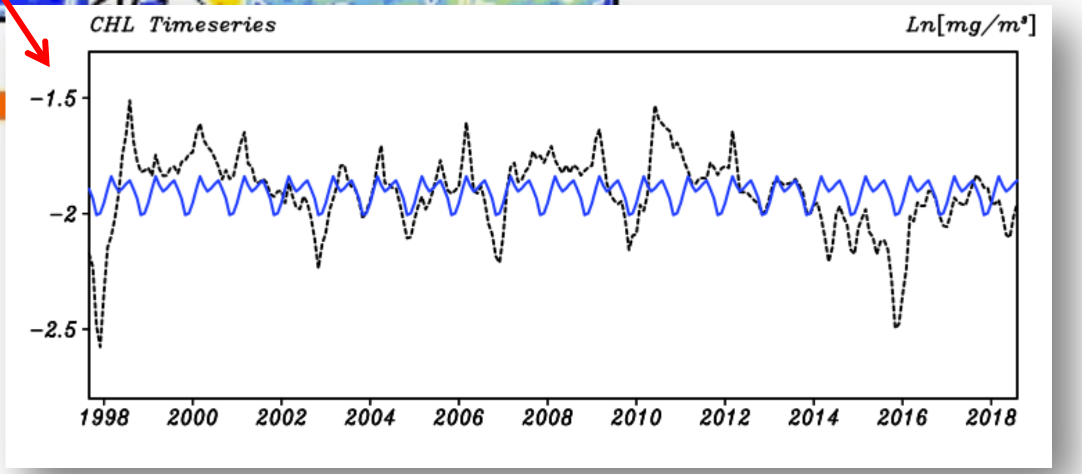

✓ Strong influence of interannual variability on TCV in tropics

Climate variability indices

Climate variability	Index	SSTa index domain	Reference
Eastern Pacific (Cold Tongue) ENSO	**NINO3**	(5°N–5°S, 150°W–90°W)	Trenberth (1997); Kug et al. (2009); Yeh et al. (2009)
Central Pacific (Warmpool) ENSO	**NINO4**	(5°N–5°S, 160°E–150°W)	
Pacific Decadal Oscillation	**PDO**	EOF 1st PC (120°E–60°W, 20°N–60°N)	Mantua et al. (1997)
North Pacific Gyre Oscillation (Victoria Mode)	**NPGO**	EOF 2nd PC (120°E–60°W, 20°N–60°N)	Bond et al. (2003); Di Lorenzo et al. (2008)
Atlantic Niño	**ATL3**	(20°W–0°, 3°S–3°N)	Zebiak (1993); Vallès-Casanova et al. (2020)
Atlantic Meridional Mode	**AMM**	(5°–15°N, 50°–20°W) minus (5°–15°S, 20°W–10°E)	Xie and Carton (2004); Doi et al. (2010)
Indian Ocean Dipole Mode	**DMI**	(50°E–70°E, 10°S–10°N) minus (90°E–110°E,10°S–0°)	Saji et al. (1999)
Indian Ocean Basin Mode	**IOBM**	(20°S–20°N, 40°–105°E)	Klein et al. (1999); Hong et al. (2010)

Thanks to Young-Ji Joh (NOAA-GFDL), Sang-Ki Lee (NOAA-AOML)

Chlorophyll reconstruction

$\boldsymbol{\tau}$: Lagged time scales of seasonal climate indices
$\boldsymbol{\beta}$: Partial Regression coefficients
"Leave One out Cross-validated"

$$\boldsymbol{rCHLa_t} = \sum_{\boldsymbol{\tau}=0}^{4}\left(\boldsymbol{\beta}_{1,\boldsymbol{t-\tau}} \cdot \boldsymbol{NINO}3_{\boldsymbol{t-\tau}} + \boldsymbol{\beta}_{2,\boldsymbol{t-\tau}} \cdot \boldsymbol{NINO}4_{\boldsymbol{t-\tau}} + \boldsymbol{\beta}_{3,\boldsymbol{t-\tau}} \cdot \boldsymbol{PDO}_{\boldsymbol{t-\tau}} + \boldsymbol{\beta}_{4,\boldsymbol{t-\tau}} \cdot \boldsymbol{NPGO}_{\boldsymbol{t-\tau}} + \boldsymbol{\beta}_{5,\boldsymbol{t-\tau}} \cdot \boldsymbol{ATL}3_{\boldsymbol{t-\tau}} + \boldsymbol{\beta}_{6,\boldsymbol{t-\tau}} \cdot \boldsymbol{AMM}_{\boldsymbol{t-\tau}} + \boldsymbol{\beta}_{7,\boldsymbol{t-\tau}} \cdot \boldsymbol{IOBM}_{\boldsymbol{t-\tau}} + \boldsymbol{\beta}_{8,\boldsymbol{t-\tau}} \cdot \boldsymbol{DMI}_{\boldsymbol{t-\tau}}\right)$$

$$\boldsymbol{rTCV} = \frac{1}{\boldsymbol{n}}\sum_{\boldsymbol{t}=1}^{\boldsymbol{n}}\left(\boldsymbol{rCHLa_t} + \boldsymbol{CHL\_SC_t} - \boldsymbol{\mu}\right)^2$$

$\boldsymbol{n}$: degree of freedom #292
$\boldsymbol{\mu}$: Chlorophyll annual mean
$\boldsymbol{CHL\_SC}$: Chlorophyll seasonal cycle

Reconstructed TCV

Case 1)

Seasonal Cycle

41.6%

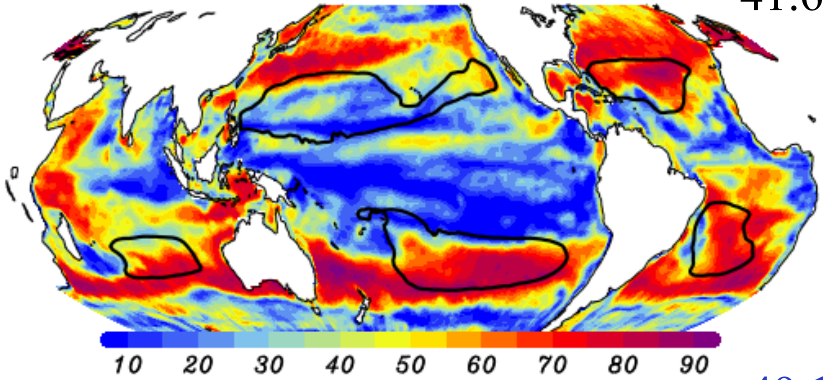

Case 2)

Seasonal Cycle

+

Instantaneous climate modes

49.1%

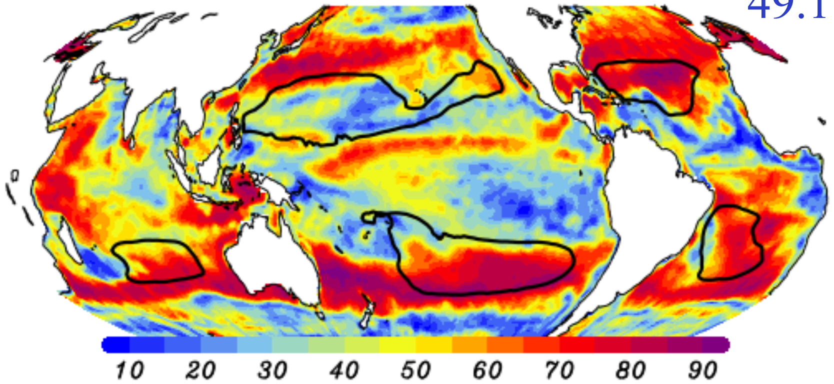

Case 3)

Seasonal Cycle

+

Instantaneous climate modes

+

Delayed climate modes

61.1%

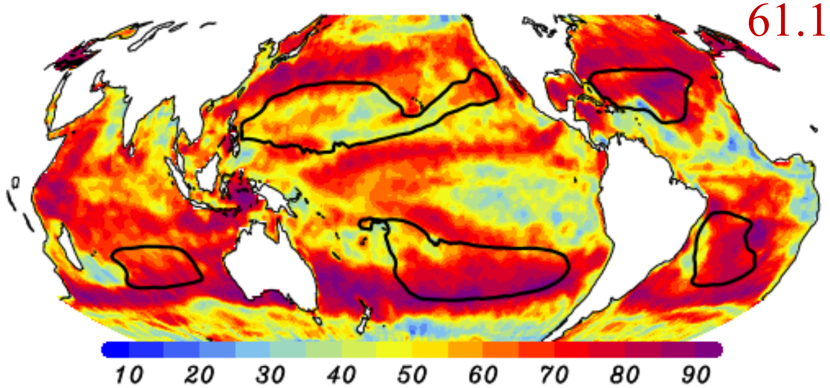

Delayed climate impacts on CHL anomaly

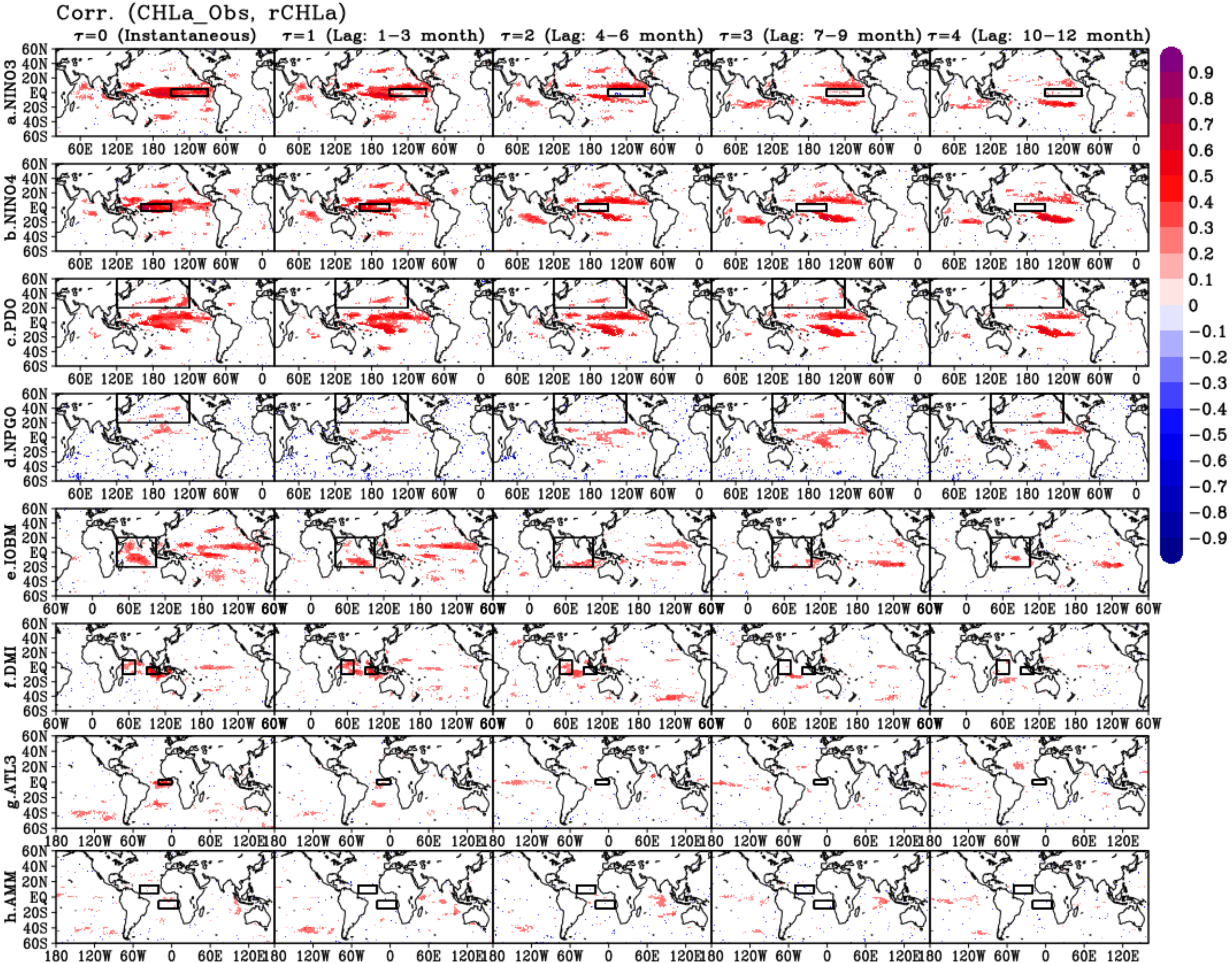

*Memory effects of ocean climate variability ~ 12 months

1) Evolution of climate variability itself
2) Pacific meridional mode
3) Inter-basin ocean influences

Reconstructed CHL anomaly correlation coefficient (ACC) skill

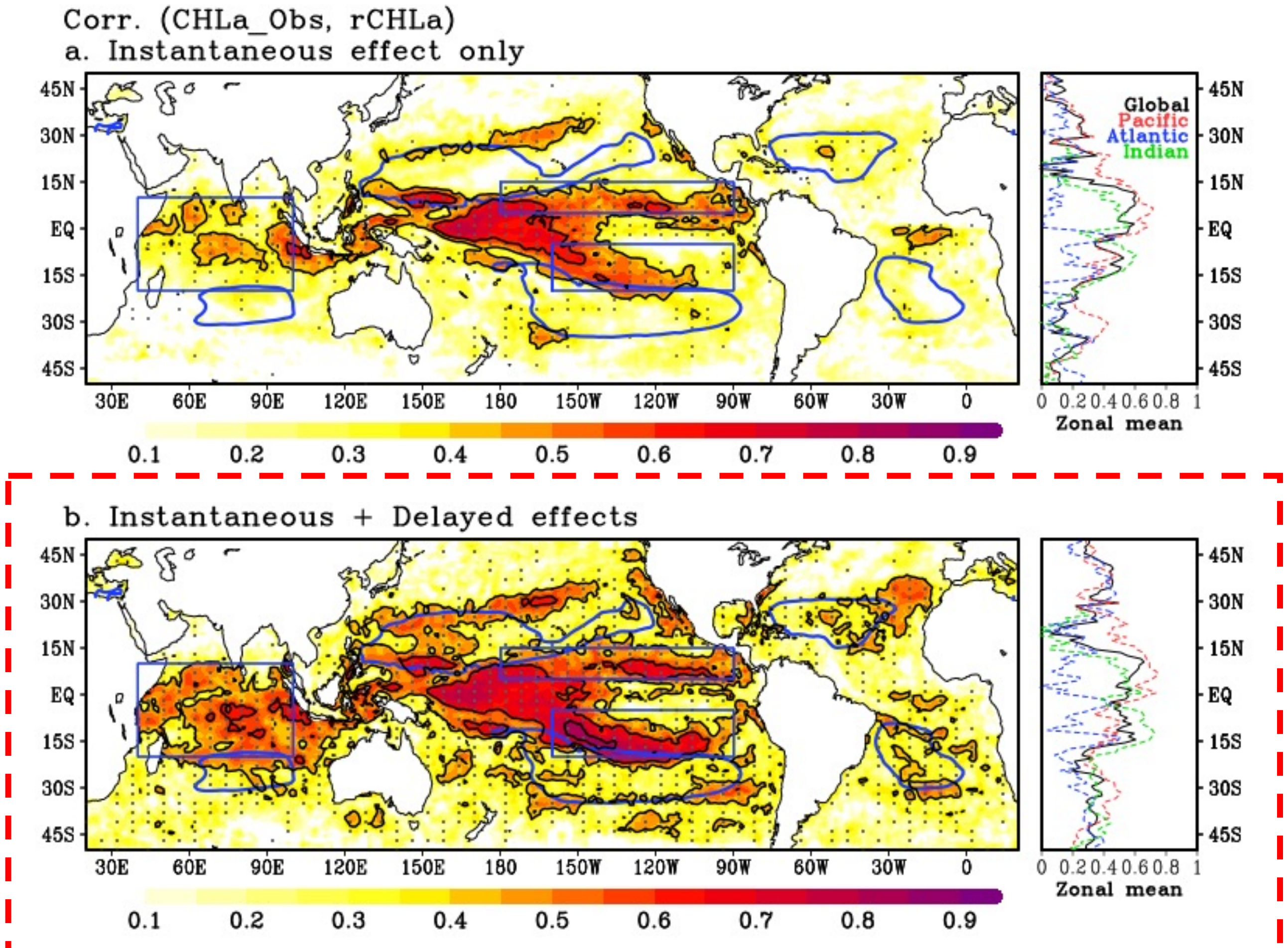

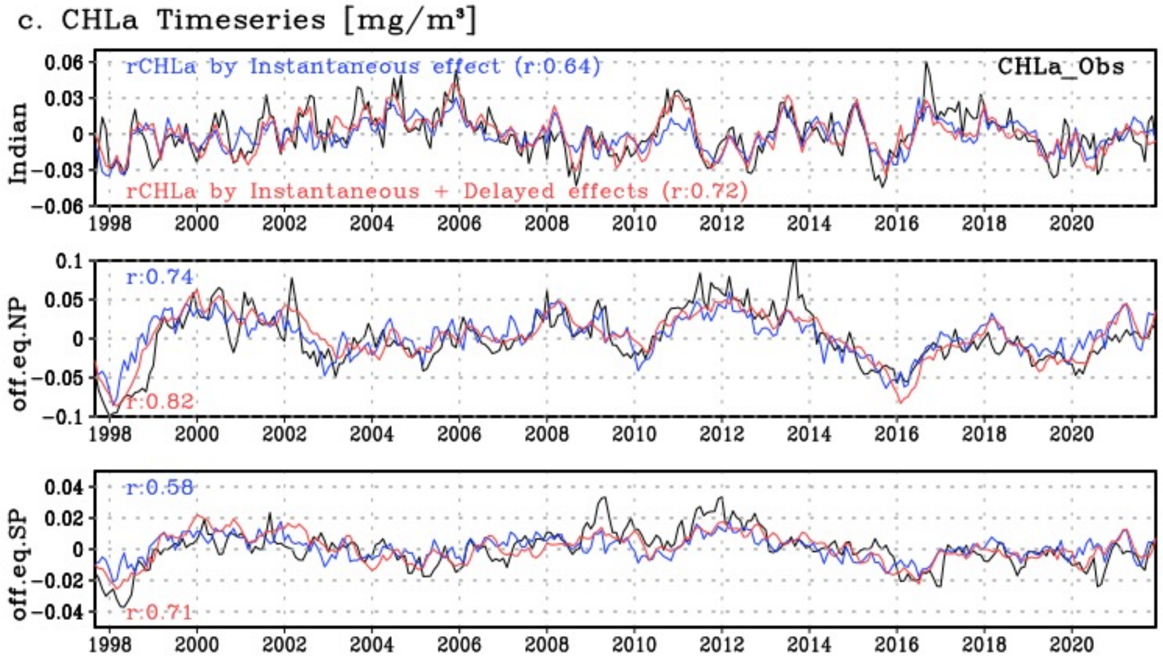

Better ACC skills

Instantaneous Climate variability -> 0.64, 0.74, 0.58

*Delayed Climate variability -> 0.72, 0.82, 0.71

CHL anomaly predictability driven by delayed climate variabilities

Dynamical Modeling prediction

A Chlorophyll Prediction Skill (Lead Time: 1-3 mon)

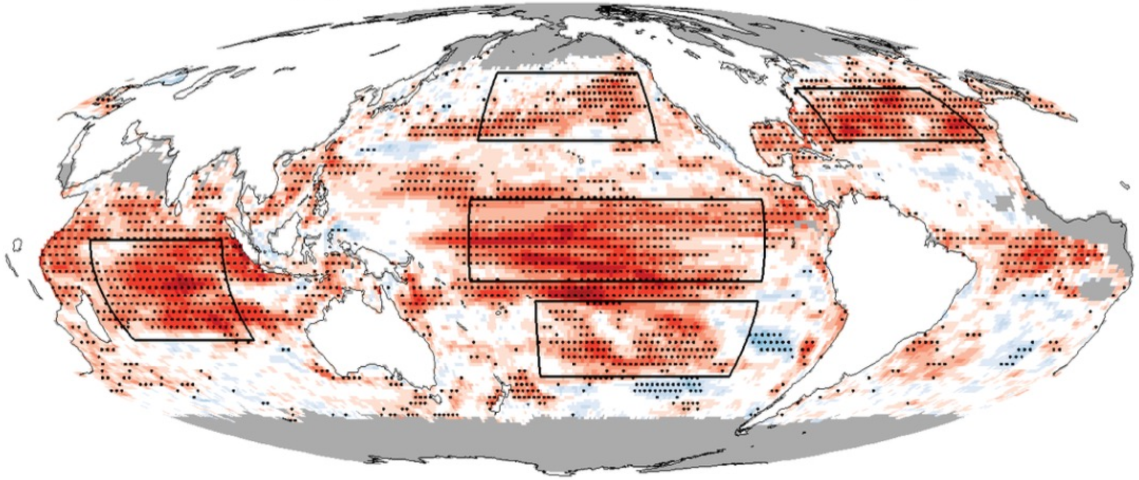

Park et al 2019

CHL anomaly predictability driven by delayed climate variabilities

Dynamical Modeling prediction

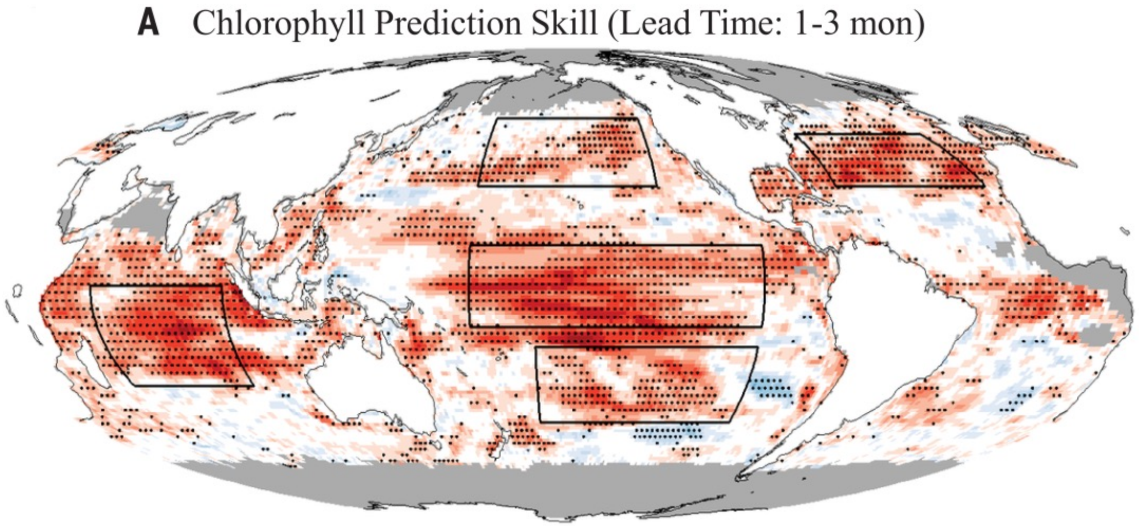

Park et al 2019

$$\boldsymbol{rCHLa_{t}\_predic} = \sum_{\tau=1}^{4}\left(\boldsymbol{\beta}_{1,t-\tau} \cdot \boldsymbol{NINO3}_{t-\tau} + \boldsymbol{\beta}_{2,t-\tau} \cdot \boldsymbol{NINO4}_{t-\tau} + \boldsymbol{\beta}_{3,t-\tau} \cdot \boldsymbol{PDO}_{t-\tau} + \boldsymbol{\beta}_{4,t-\tau} \cdot \boldsymbol{NPGO}_{t-\tau} + \boldsymbol{\beta}_{5,t-\tau} \cdot \boldsymbol{ATL3}_{t-\tau} + \boldsymbol{\beta}_{6,t-\tau} \cdot \boldsymbol{AMM}_{t-\tau} + \boldsymbol{\beta}_{7,t-\tau} \cdot \boldsymbol{IOBM}_{t-\tau} + \boldsymbol{\beta}_{8,t-\tau} \cdot \boldsymbol{DMI}_{t-\tau}\right)$$

CHL anomaly predictability driven by delayed climate variabilities

Dynamical Modeling prediction

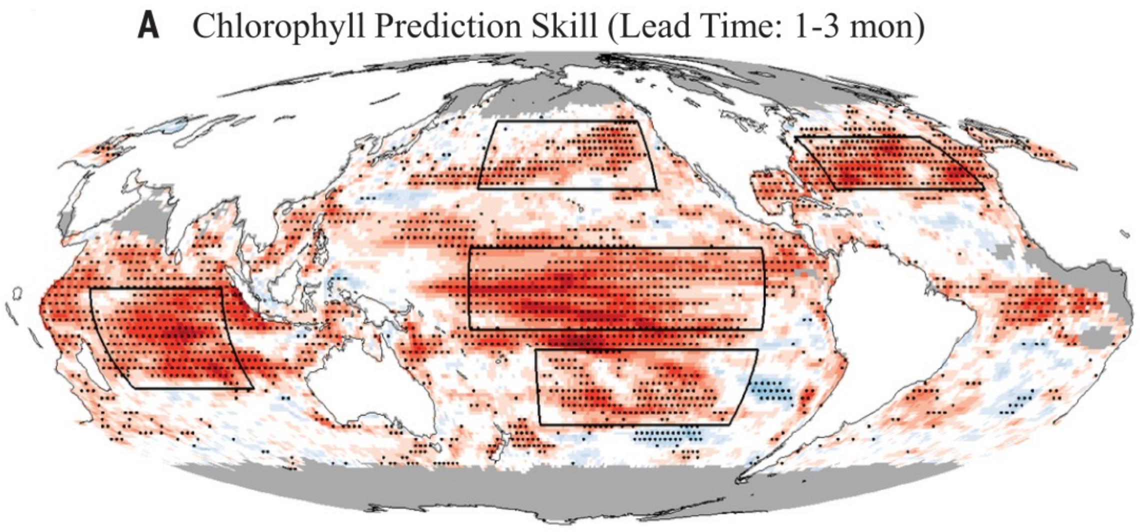

Park et al 2019

$$rCHLa_{t}\_predic = \sum_{\tau=1}^{4}\left(\beta_{1,t-\tau}\cdot NINO3_{t-\tau} + \beta_{2,t-\tau}\cdot NINO4_{t-\tau} + \beta_{3,t-\tau}\cdot PDO_{t-\tau} + \beta_{4,t-\tau}\cdot NPGO_{t-\tau} + \beta_{5,t-\tau}\cdot ATL3_{t-\tau} + \beta_{6,t-\tau}\cdot AMM_{t-\tau} + \beta_{7,t-\tau}\cdot IOBM_{t-\tau} + \beta_{8,t-\tau}\cdot DMI_{t-\tau}\right)$$

Statistical Modeling prediction

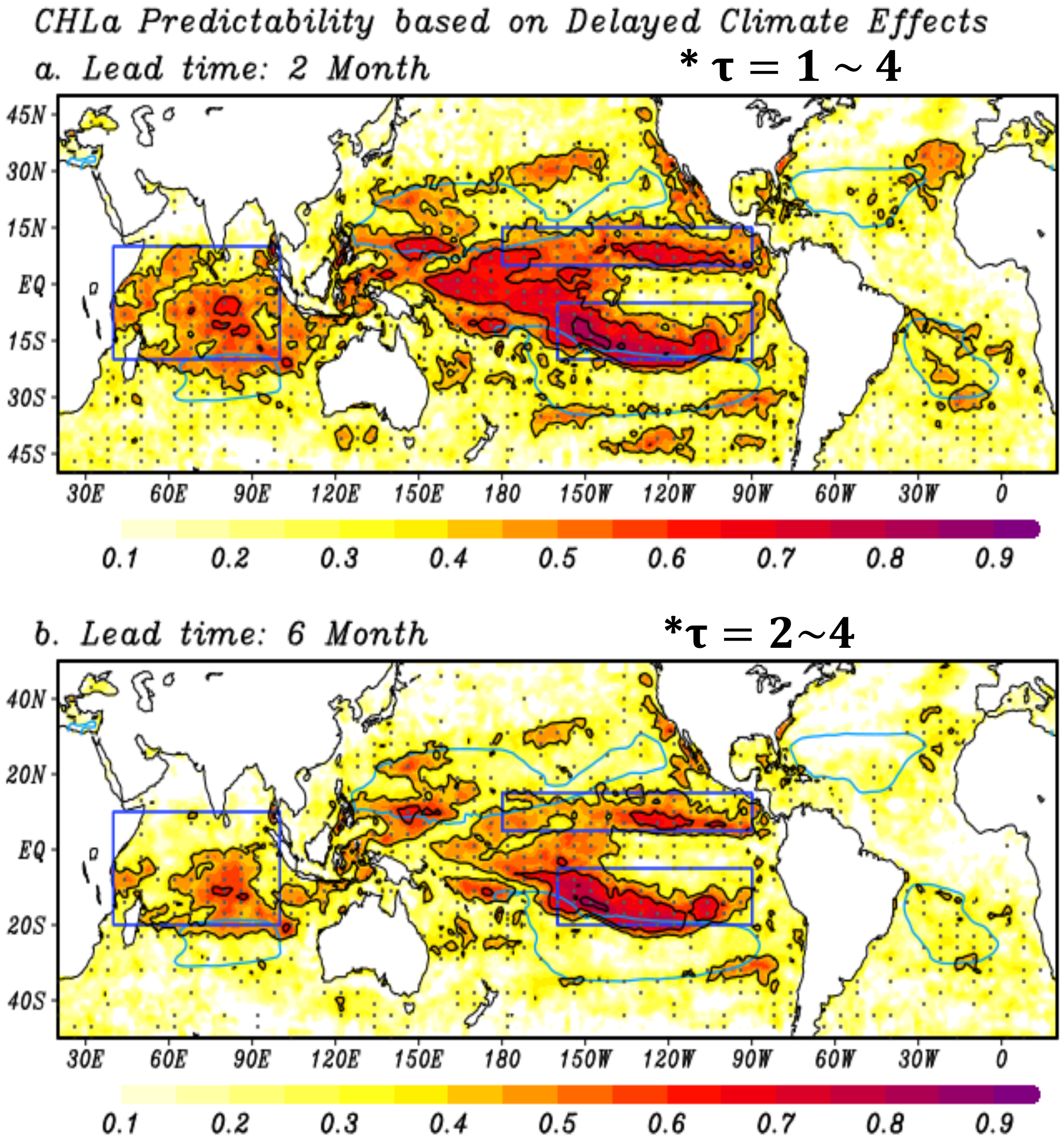

Summary

Attribution of Total Chlorophyll Variance (%)

Case 1)

Seasonal Cycle

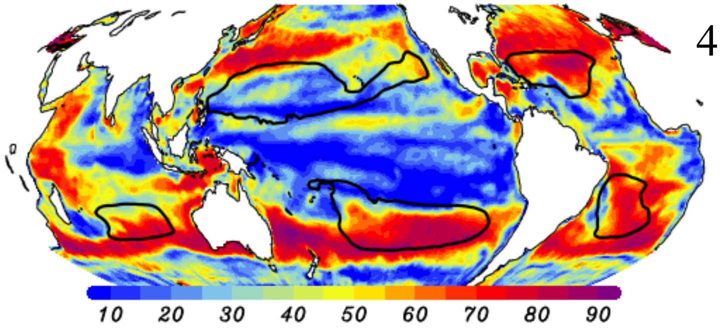

41.6%

Case 2)

Seasonal Cycle

+

Instantaneous climate modes

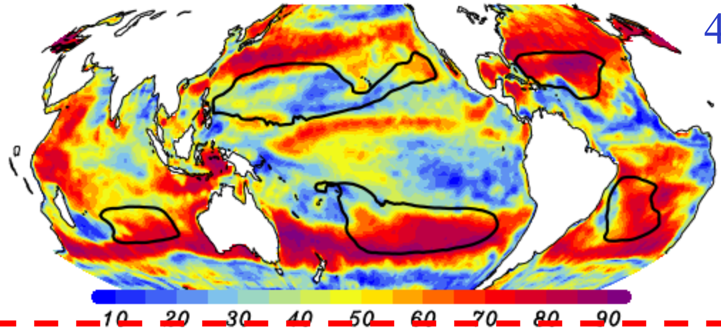

49.1%

Case 3)

Seasonal Cycle

+

Instantaneous climate modes

+

Delayed climate modes

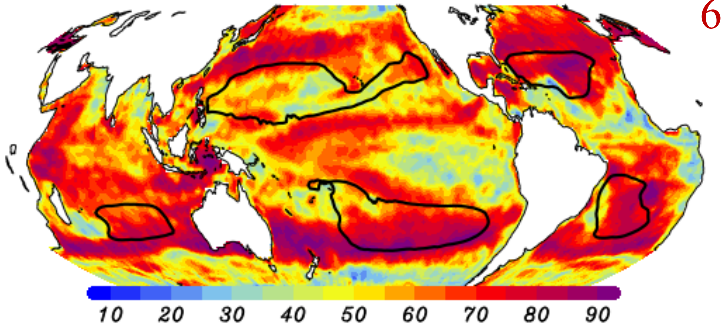

61.1%

***Critical source in chlorophyll variance and predictability**

Challenging points for residual (39%)

- Internal biogeochemical processes
- Mesoscale eddy
- Volcanic eruption
- Sea ice
- Stochastic atmospheric variabilities

Future work

- CMIP6 ESMs assessment
- Chemical dissolved matter (CDM), pCO_2, CO_2flux, and other BGC variables
- SST based hybrid chlorophyll model

Adjusting "ocean memory effects" ~ 12 month

*Lim et al. (2022): Attribution and predictability of climate-driven variability in global ocean color. *JGR-Oceans*, 127, e2022JC019121. https://doi.org/10.1029/2022JC019121

"Poster" Post-El Nino Chlorophyll rebound in GFDL-ESM4.1

1) Oceanic Iron transport*
2) Atmospheric mineral dust

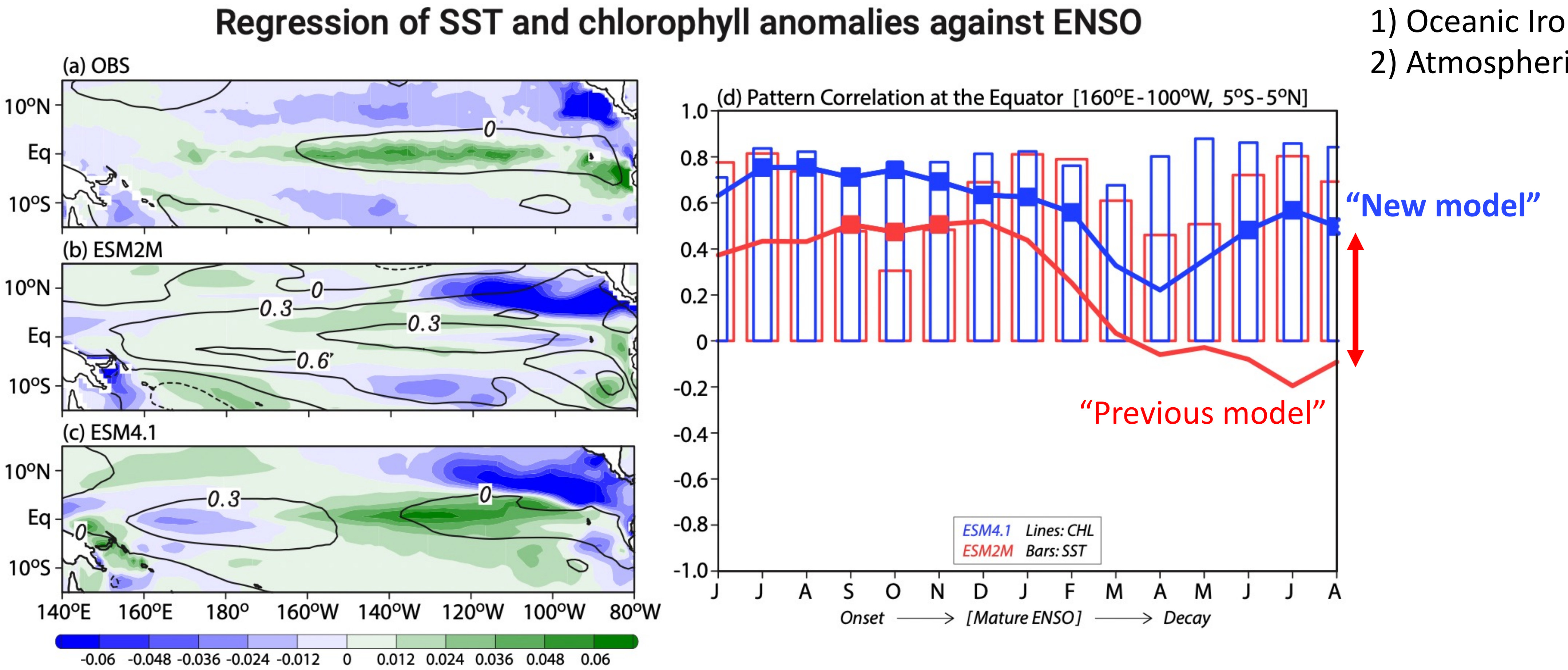

Spatially resolved ENSO-regression of temperature (contours, °C/°C) and chlorophyll concentration (shading, mgm3/°C) anomalies against ENSO in (a) satellite, Simple Ocean Data Assimilation (SODA), (b) ESM2M, and (c) ESM4.1.

Values are shown for the ENSO decay state one year after the peak (JJA+1); (d) pattern correlations of ESM2M (red) and ESM4.1 (blue) regression coefficients (i.e., panels (b) and (c)) with SODA (bars) and satellite chlorophyll (lines; square symbols denote the Student's t-test statistical significance at 95% confidence level) regression coefficients (i.e., panel (a)) in the EP (160°E–100°W, 5°N–5°S).

Lim et al 2022 GRL

Thank you

Scales of fisheries decisions related to weather & climate

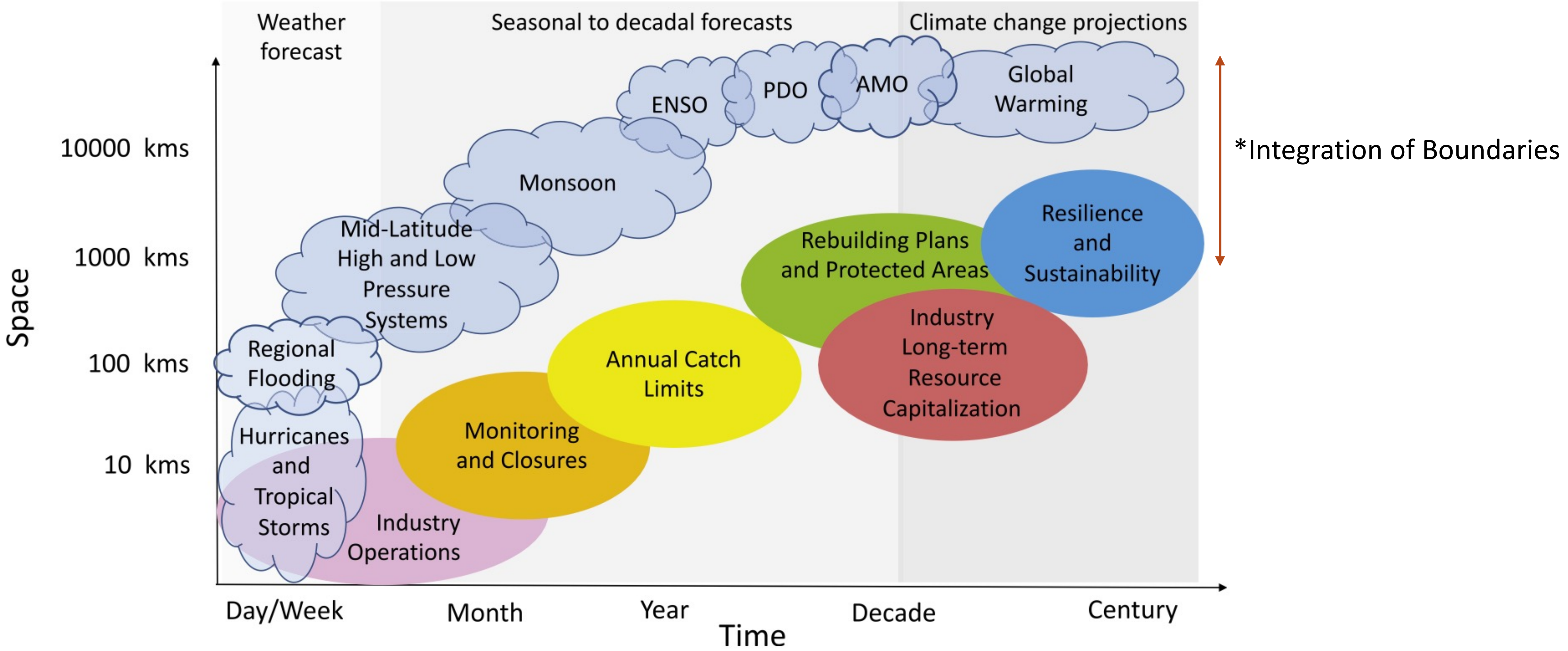

Tommasi et al 2017

Earth system model to Fisheries Size and Functional Type model (FEISTY)

NOAA - Modeling, Analysis, Predictions and Projections (MAPP) project
: Marine Ecosystem Task Force led by NOAA-PSL, NOAA-ESRL, UCSD-SIO, NOAA-GFDL

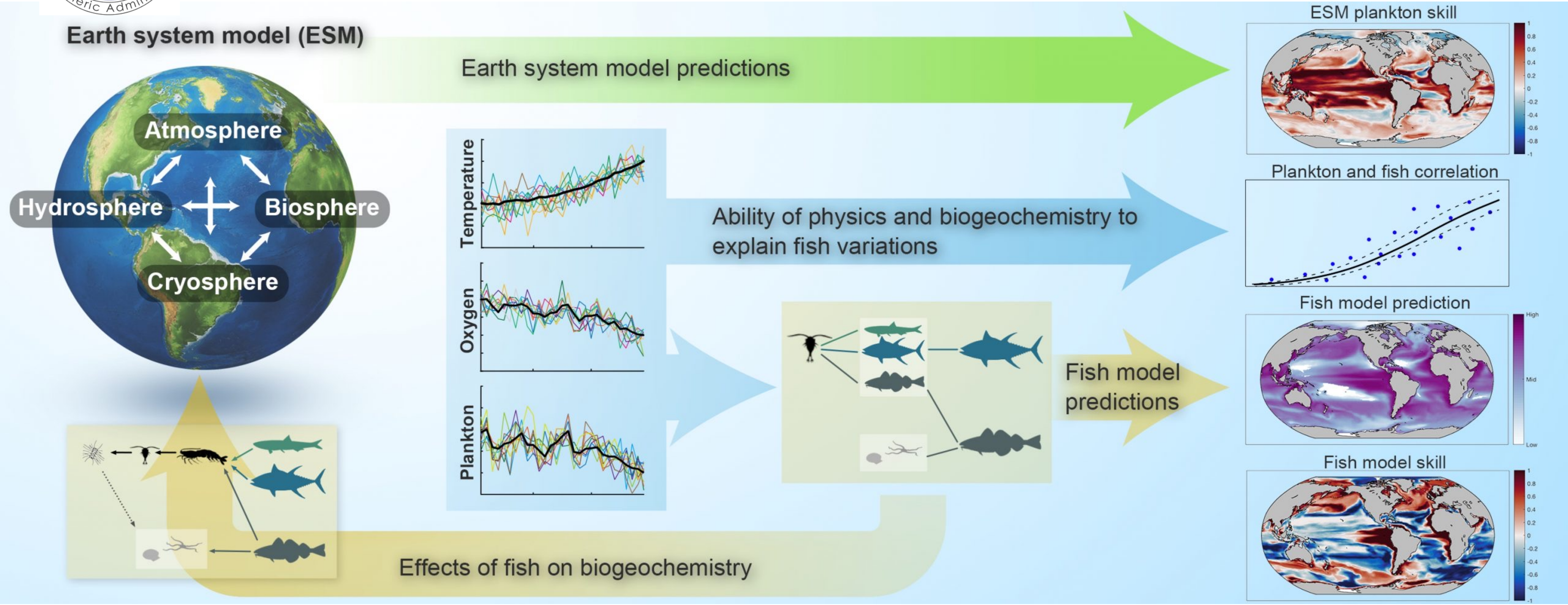

Courtesy : Colleen Petrik

Multi-year prediction of Earth system model (GFDL-ESM2M-COBALT)

Chlorophyll, Temperature, pH, Oxygen prediction

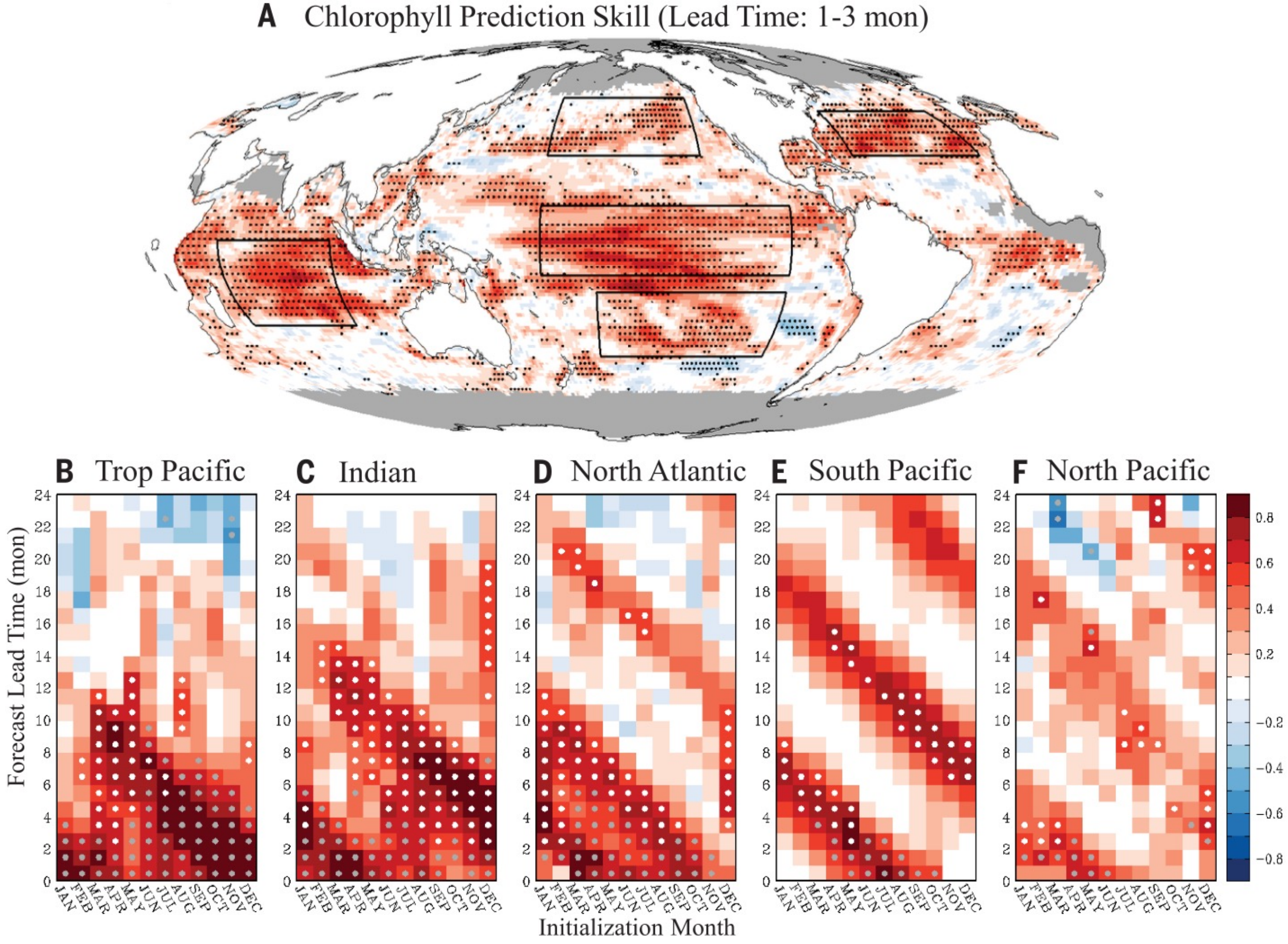

Fish catch prediction

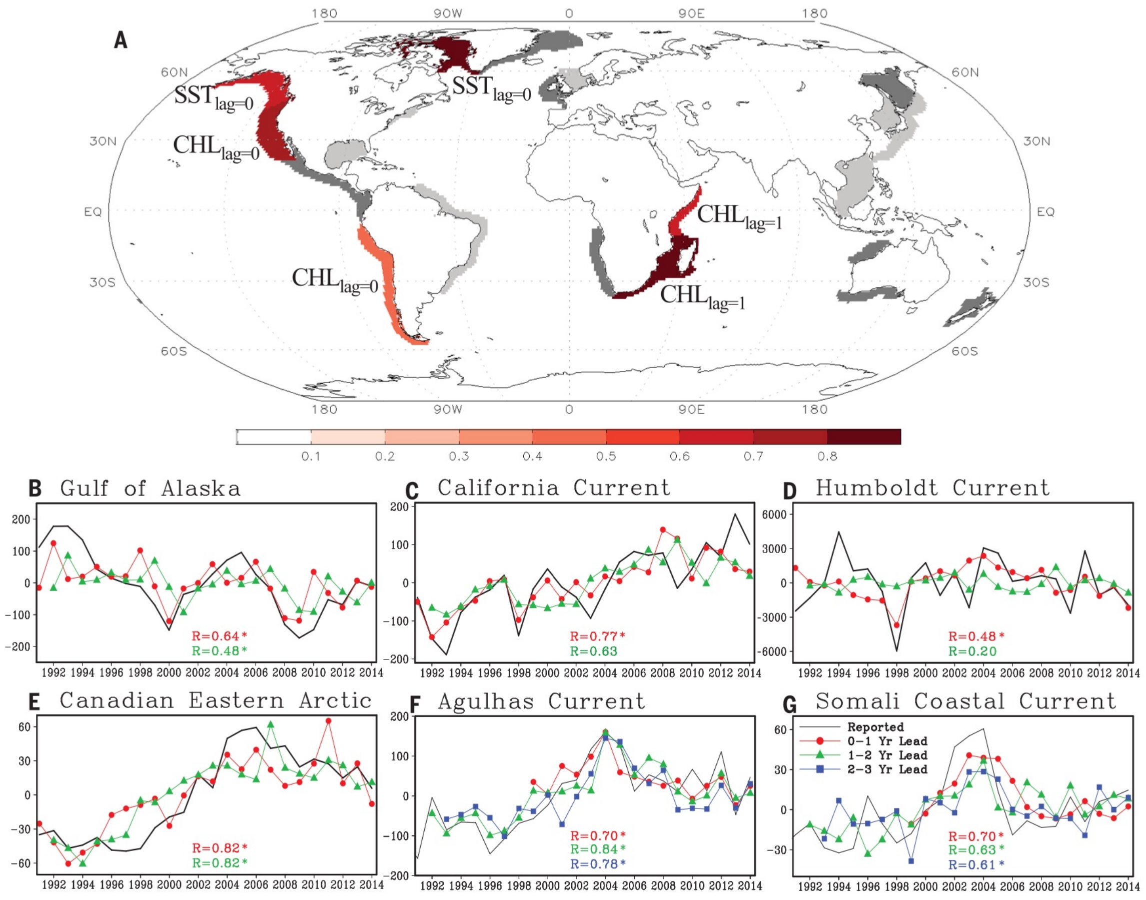

*Comprehensive fully coupled earth system model development to represent marine ecosystem variability

Park et al 2019 Science

CHL anomalies in 97/98 El Niño event

SST

SeaWiFS CHL

El Niño
Mature

+6m

El Niño
Decay

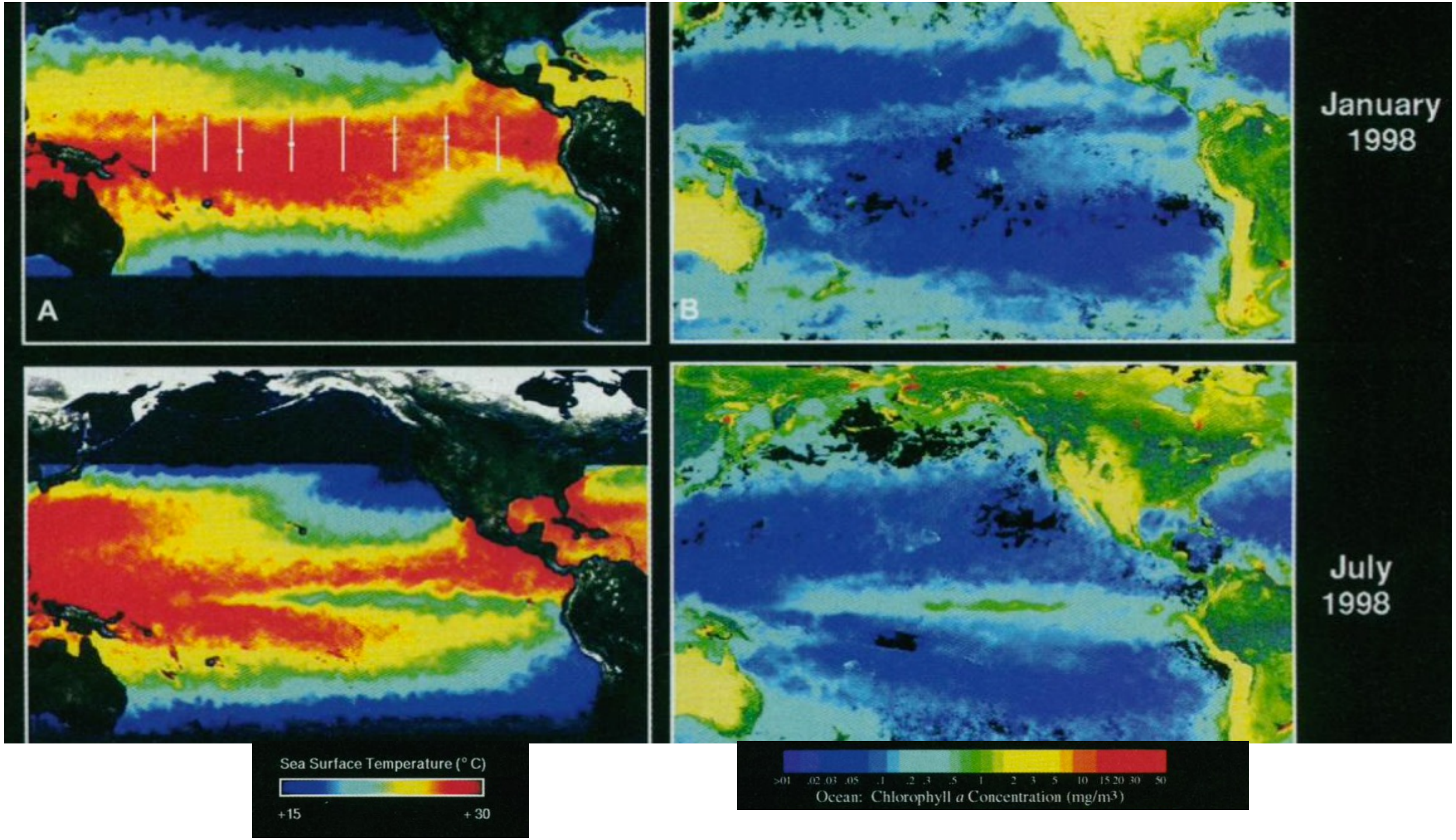

Chavez et al 1999

Primary production changes [La Niña – El Niño]

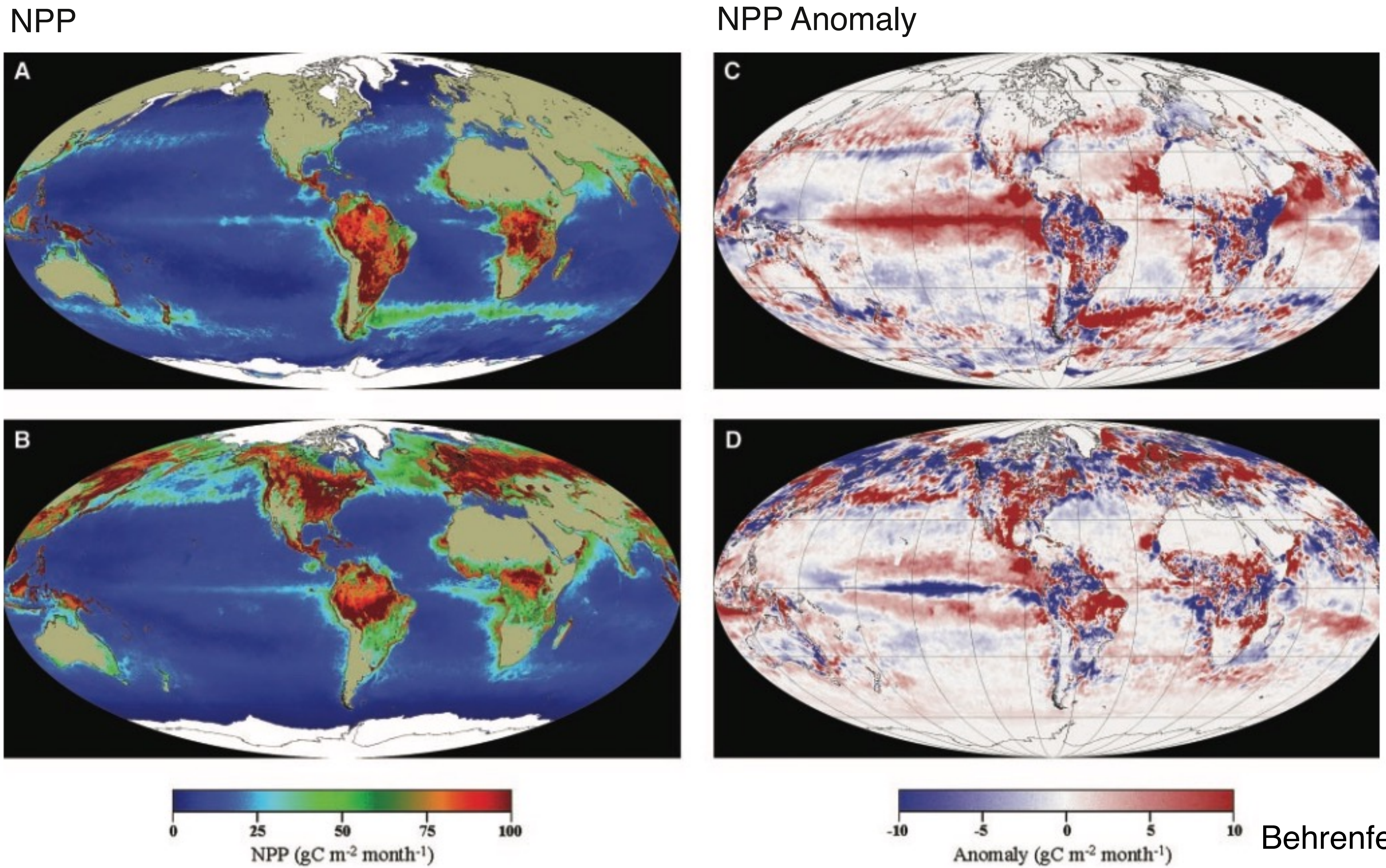

98/99 – 97/98 winter

99 - 98 Summer

Behrenfeld et al. 2001

Regression in chlorophyll against NINO3.4 index

OBS

GFDL-ESM2M

Time progress

ENSO develop
-6month

ENSO Mature
0month

ENSO Decay
+6month

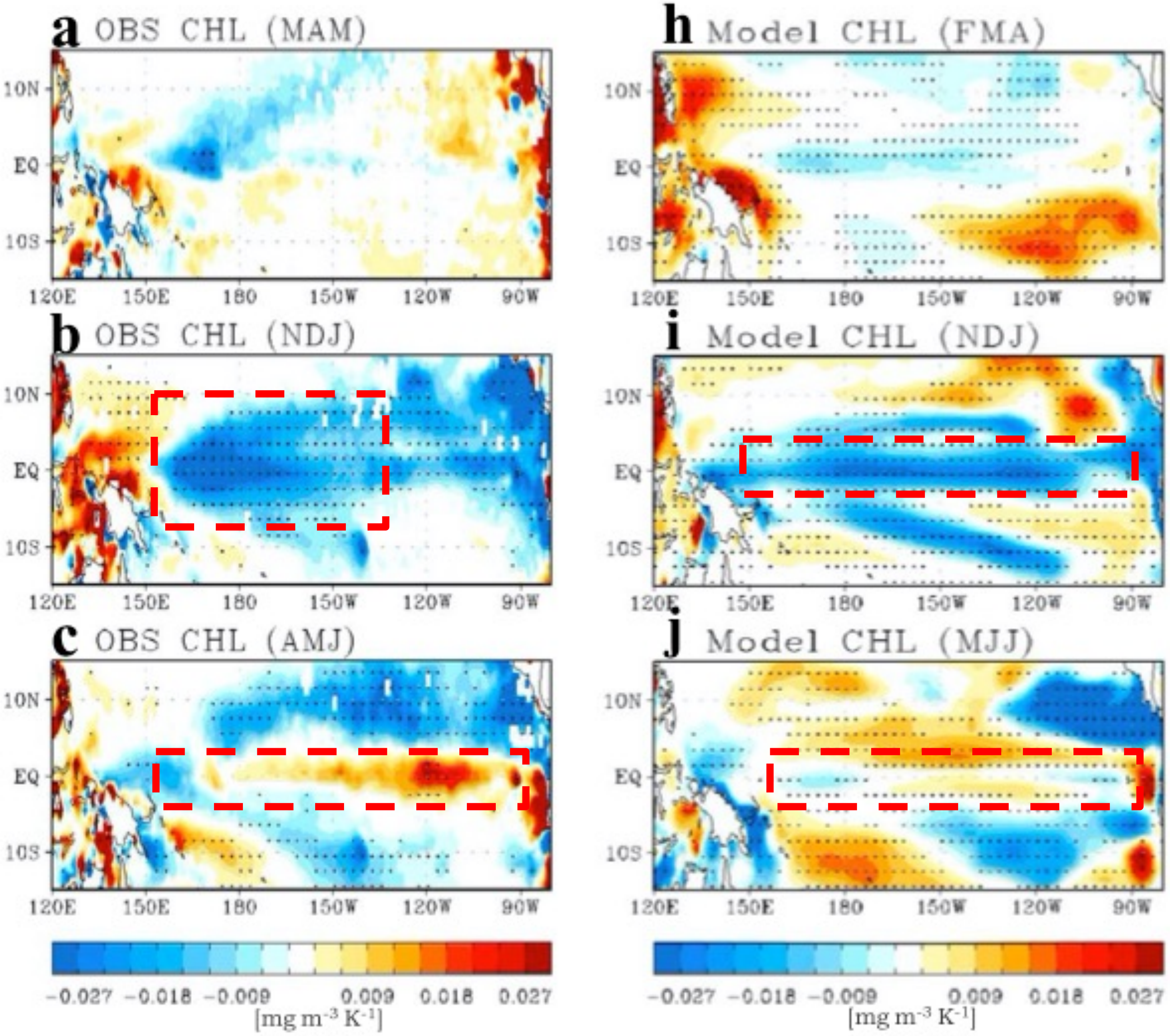

← Narrow negative CHL pattern

← Weak positive CHL at equator

Park et al. 2018 GRL

Ocean dynamics “El Niño - Southern Oscillation”

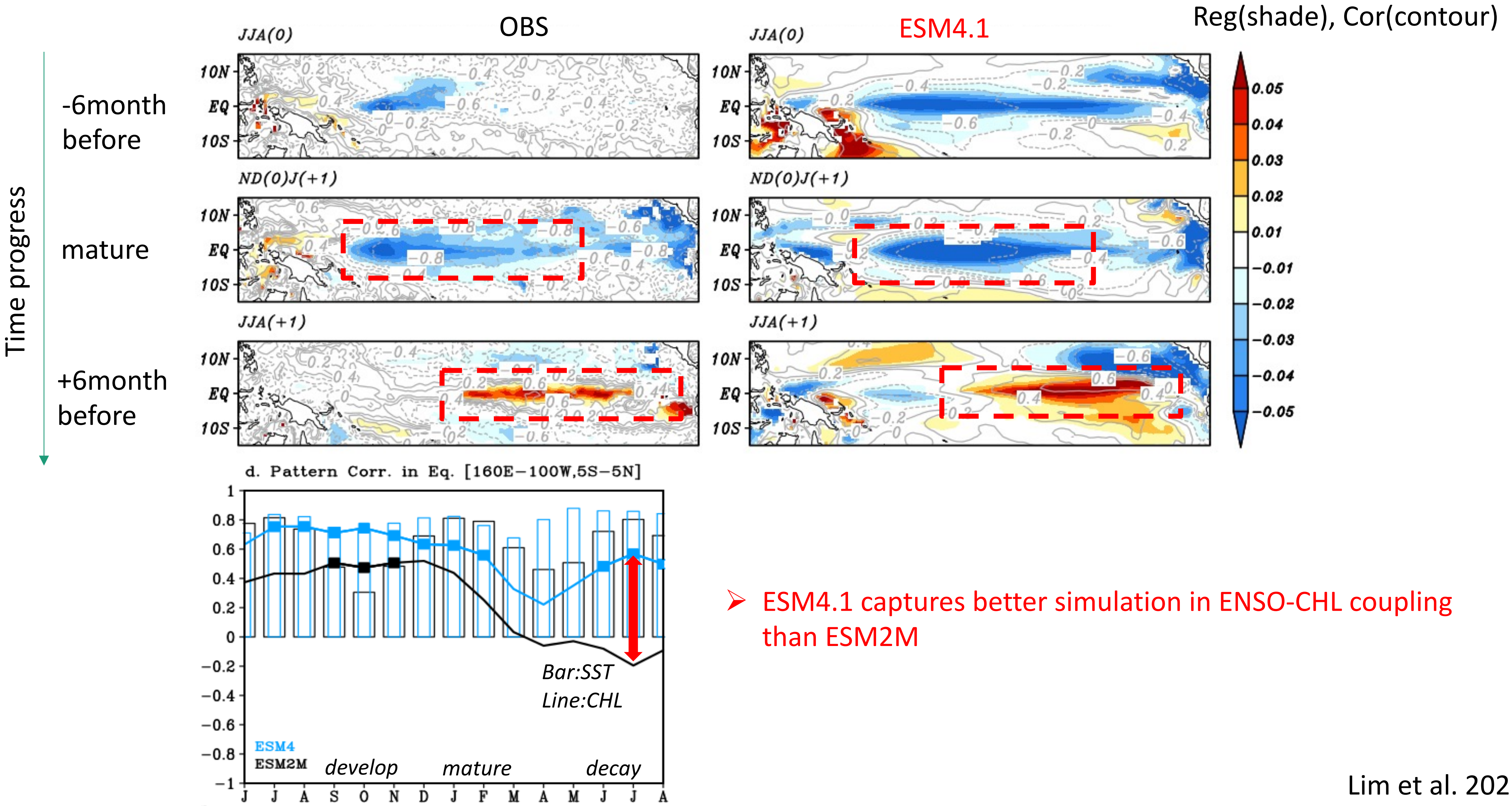

- ESM4.1 captures better simulation in ENSO-CHL coupling than ESM2M

Lim et al. 2022 GRL

Iron limitation in Tropical Pacific

Observation

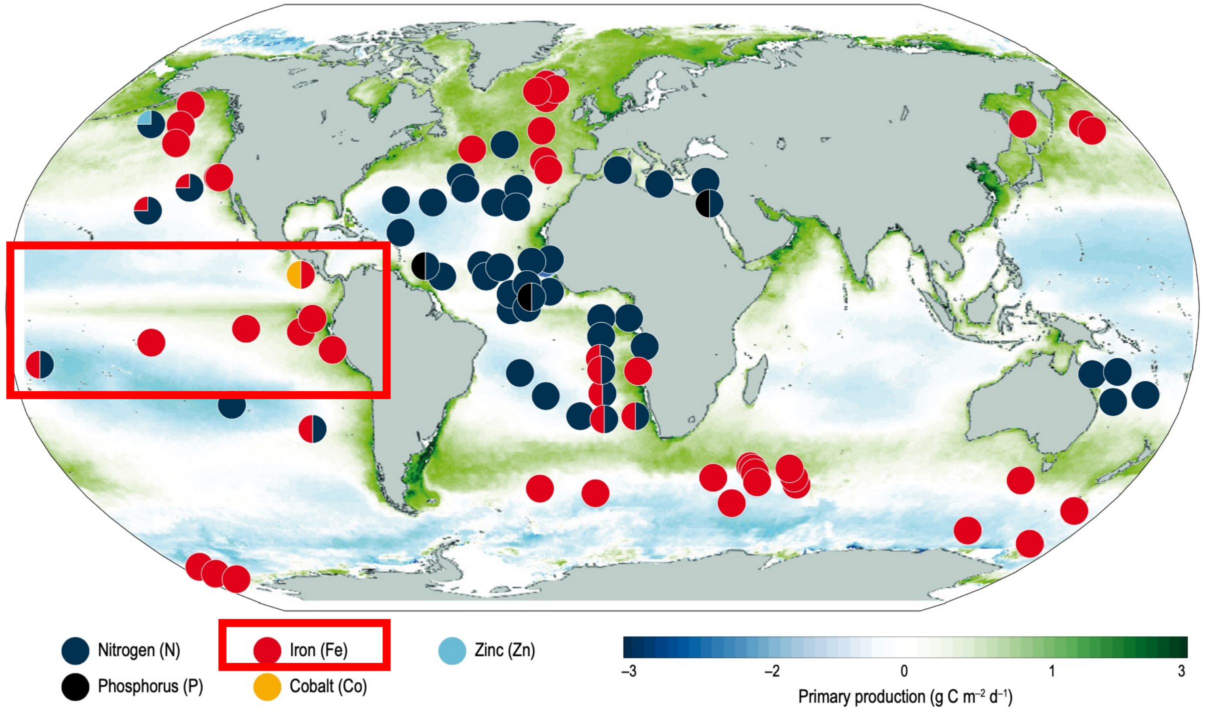

Figure 5.11 | Map of the dominant limiting resource (Moore et al. 2013), updated to include new experiments from the north Pacific, tropical Atlantic and south east Atlantic (Browning et al. 2017; Shilova et al. 2017). The background is depth integrated primary productivity using the Vertically Generalized Production Model algorithm. Colouring of the circles indicates the primary limiting nutrients inferred from chlorophyll and/or primary productivity increases following artificial amendment of: N (blue), P (black), Fe (red), Co (yellow) and Zn (cyan). Divided circles indicate potentially co-limiting nutrients, for example, a red-blue divided circle indicates Fe-N co-limitation.

GFDL-ESM4.1

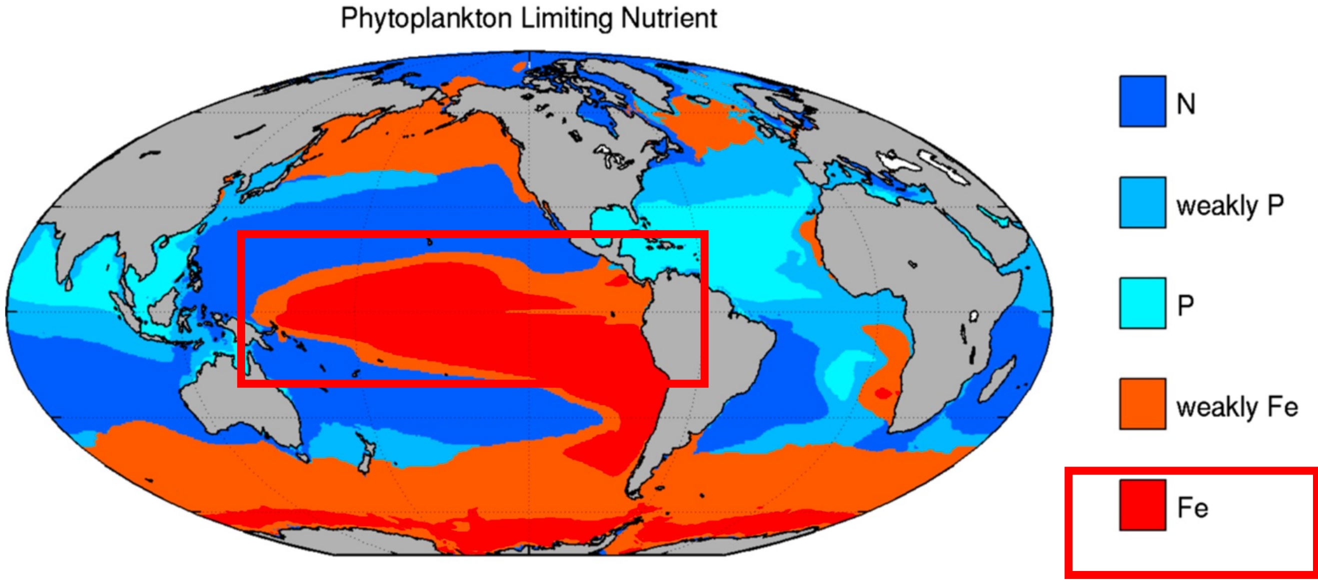

Changing Ocean, Marine Ecosystems, and Dependent Communities (IPCC Special Report on the Ocean and Cryosphere in a Changing Climate Ch.5.)

Stock et al. 2020

“Nutrient transport of ocean current”

Temperature

Dissolved Iron

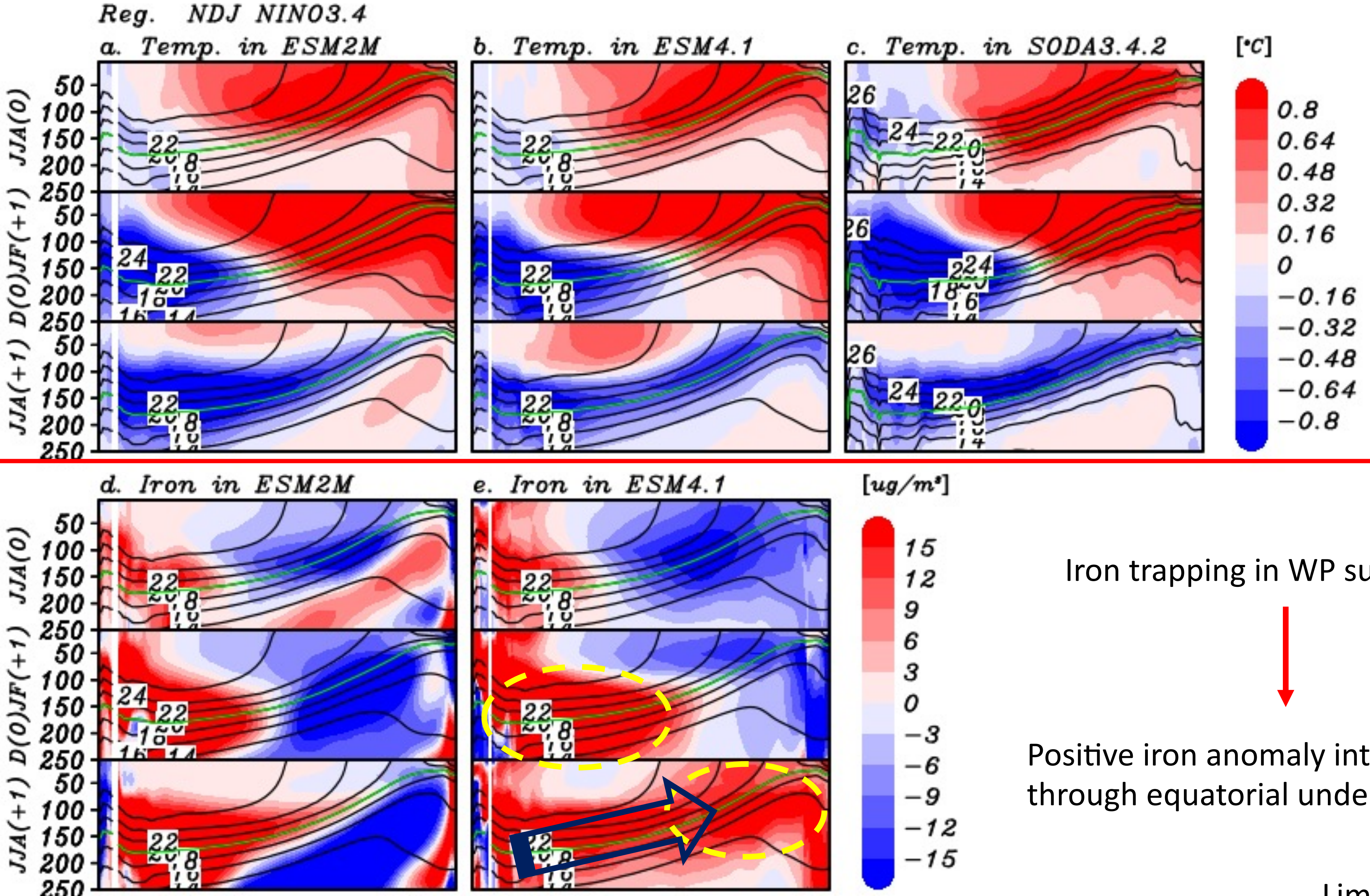

Iron trapping in WP subsurface

Positive iron anomaly into EP surface through equatorial undercurrent

Lim et al. 2022 GRL

Mineral dust: “New” iron source of ESM4.1

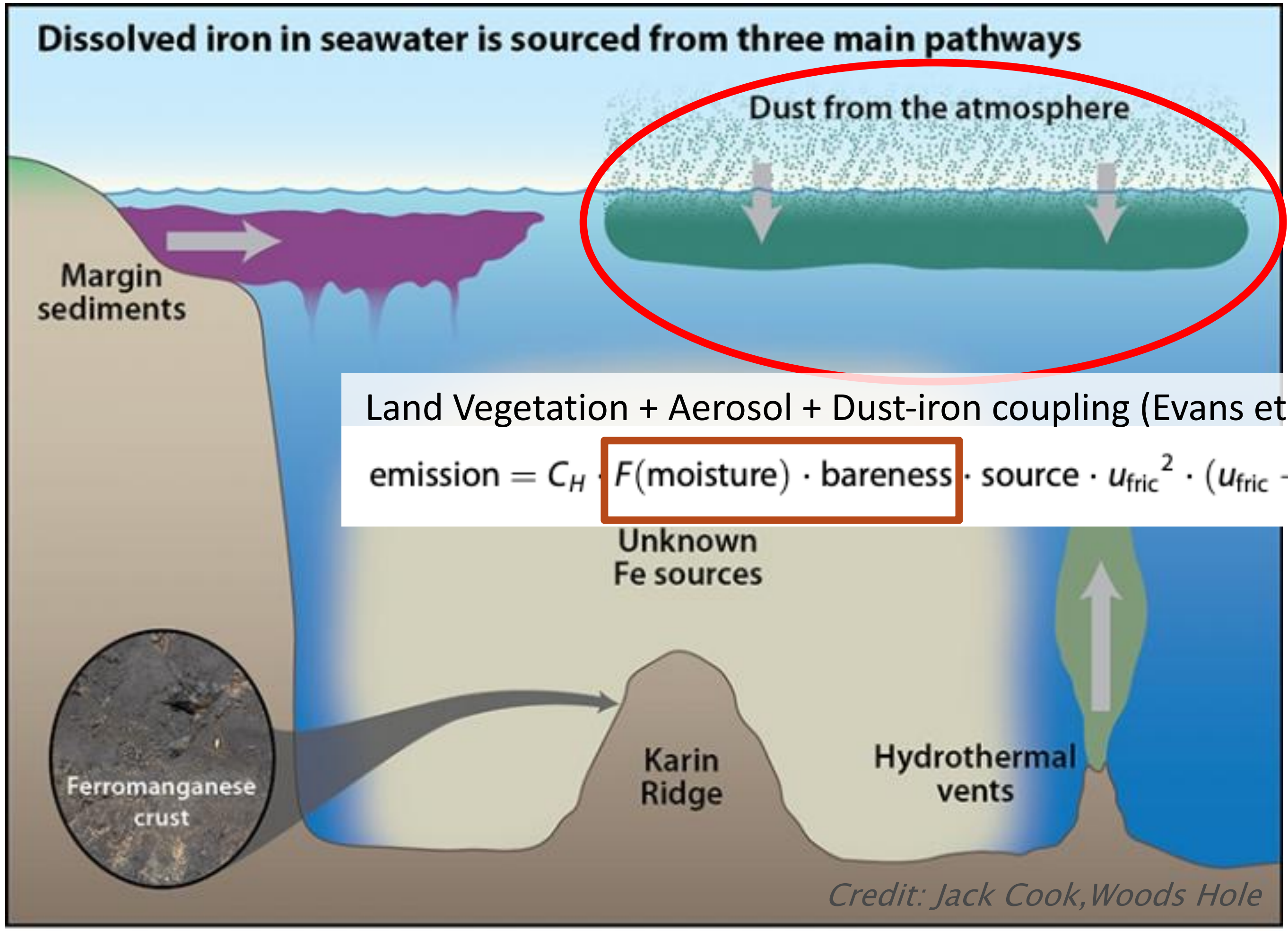

Land Vegetation + Aerosol + Dust-iron coupling (Evans et al 2016)

$$\text{emission} = C_H \cdot \boxed{F(\text{moisture}) \cdot \text{bareness}} \cdot \text{source} \cdot u_{\text{fric}}{}^2 \cdot (u_{\text{fric}} - u_{\text{thresh}})$$

Aerosol Optical Depth

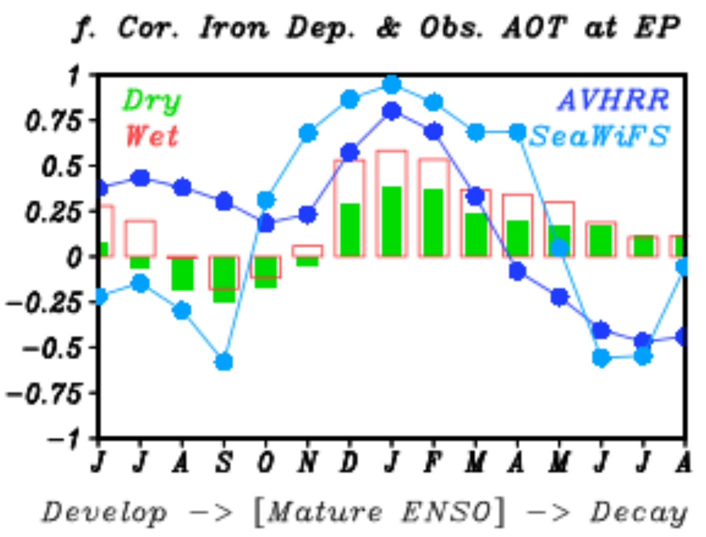

ESM4.1 Iron deposition

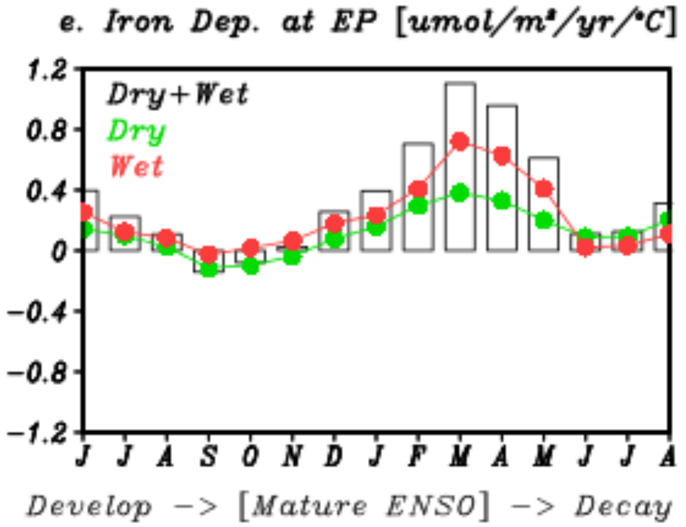

Lim et al. 2022 GRL

Regressed Precipitation, windstress and AOT in OBS

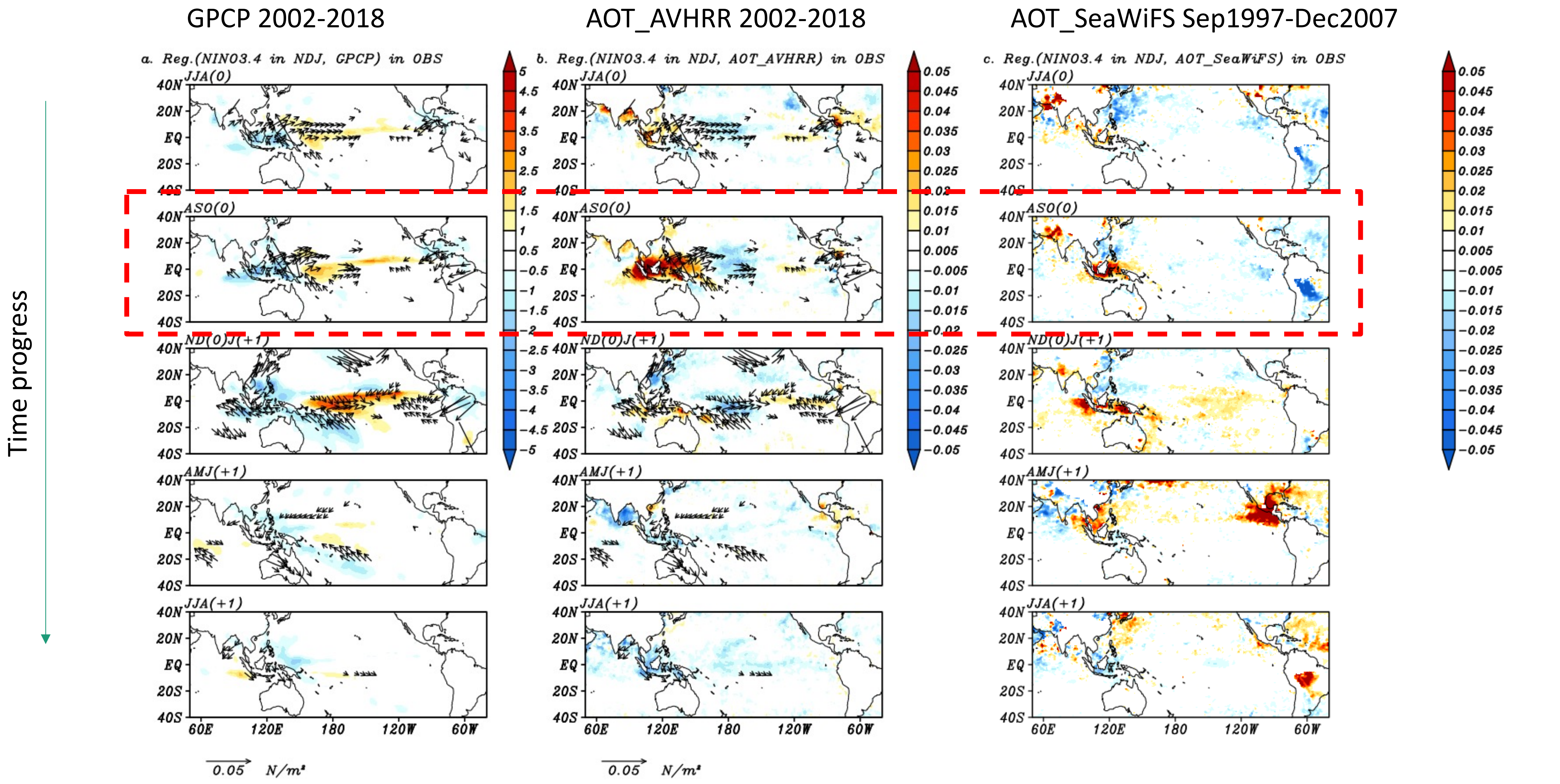

ENSO-correlated AOT response

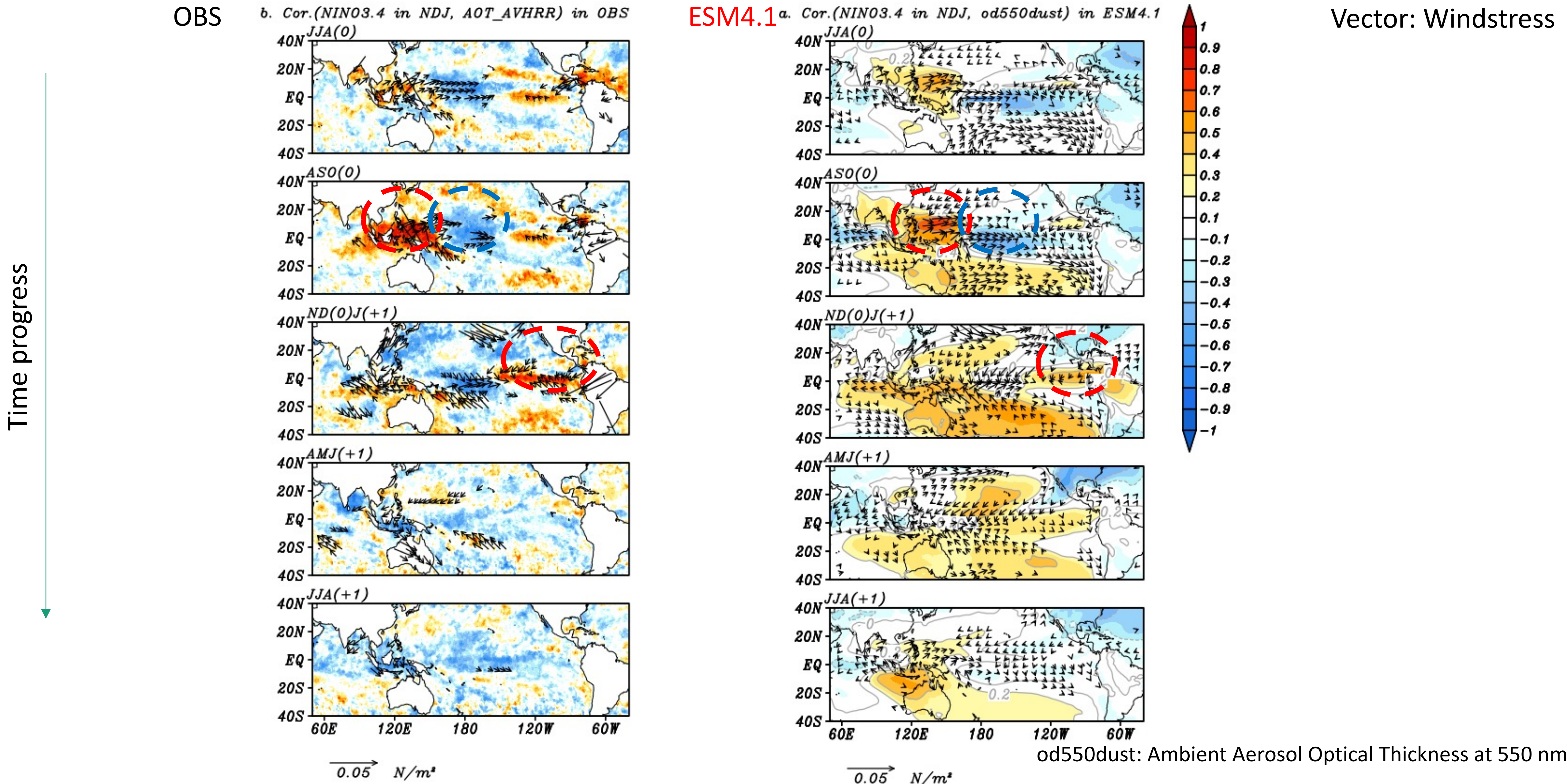

od550dust: Ambient Aerosol Optical Thickness at 550 nm

"Idealized experiment": ESM4.1-static dust-iron simulation

GFDL-ESM4.1

Impact of interannual dust-iron variability
= ESM4.1 – ESM4.1-static

ESM4.1	ESM4.1-static
Simulated dust-iron deposition	**Prescribed dust-iron deposition (monthly mean climatology in ESM4.1)**

None of interannual iron deposition variability

***Integration**

- ESM4.1: 145-yr (501-645yrs) of CMIP6 picontrol
- ESM4.1-static : 145-yr runs (501-645yrs) from 499yr initial condition of ESM4.1

Lim et al. 2022 GRL

Mineral dust coupling: Dynamic Dust effect in ESM4.1

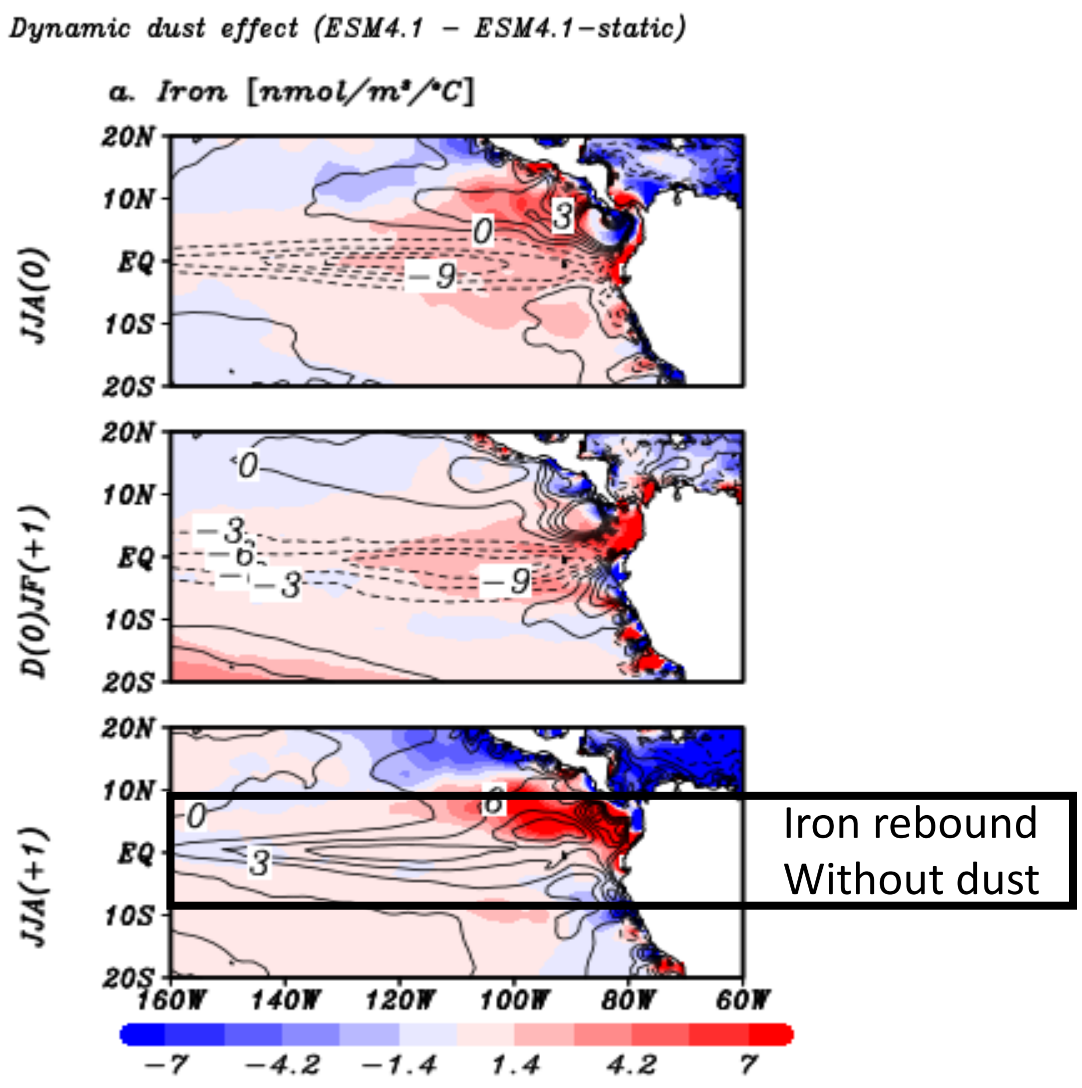

El Niño -> Dry Land -> high dust emission

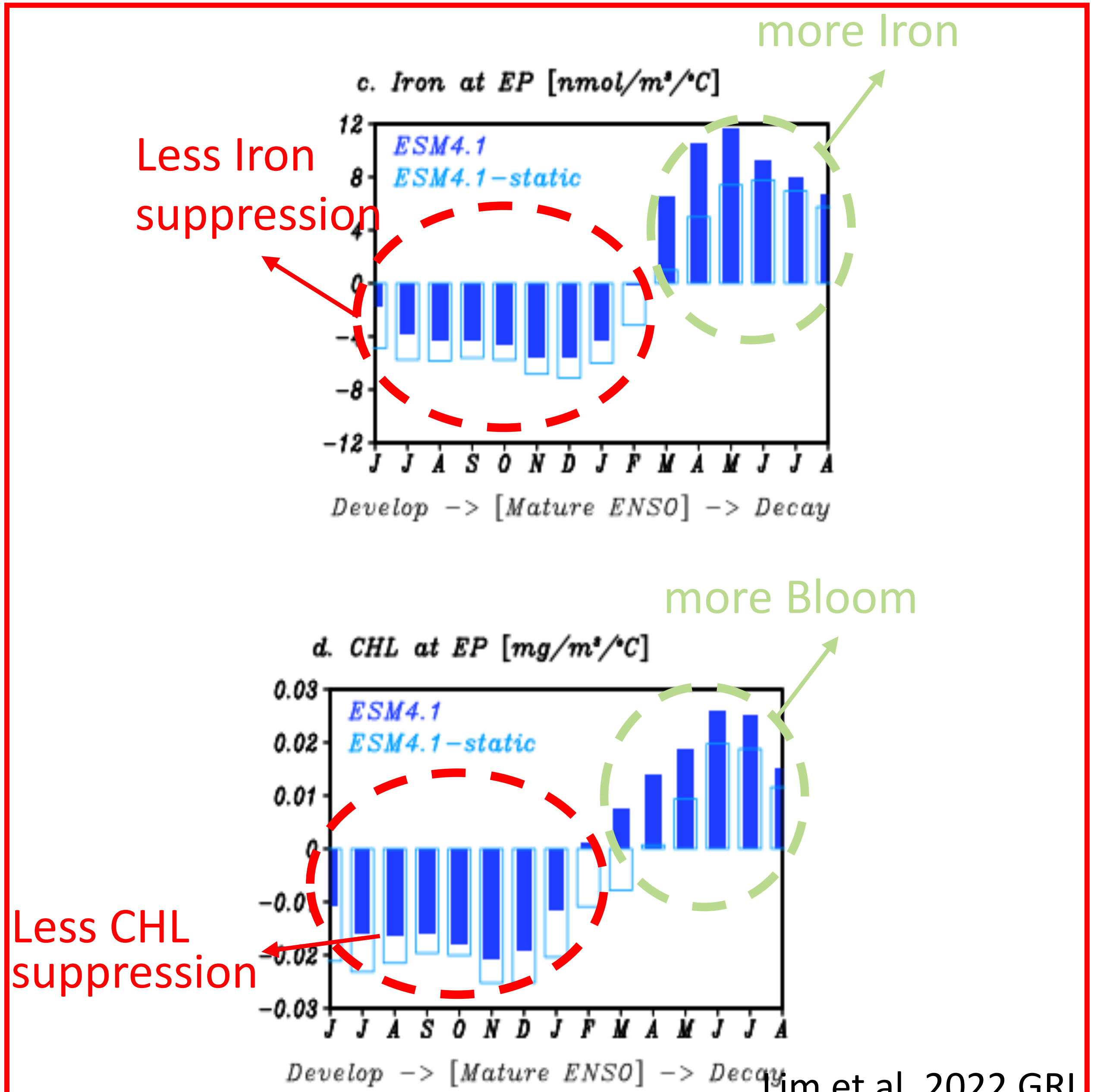

Lim et al. 2022 GRL

Summary II

CHL

Iron

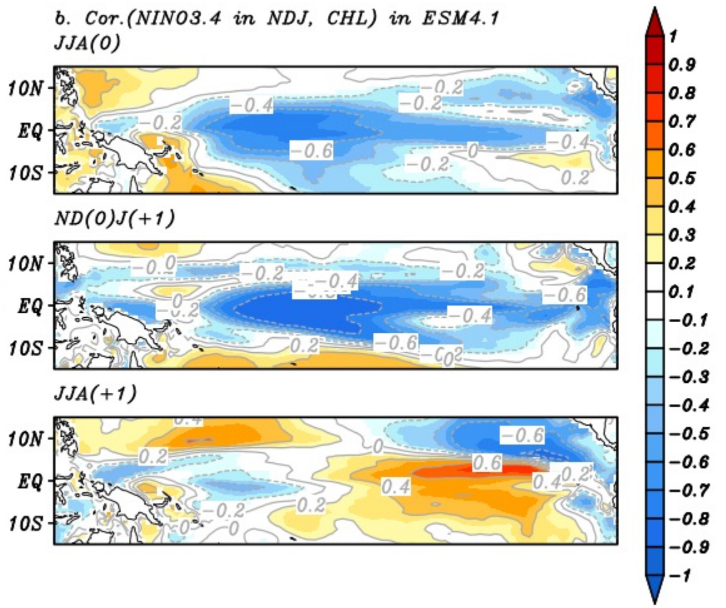

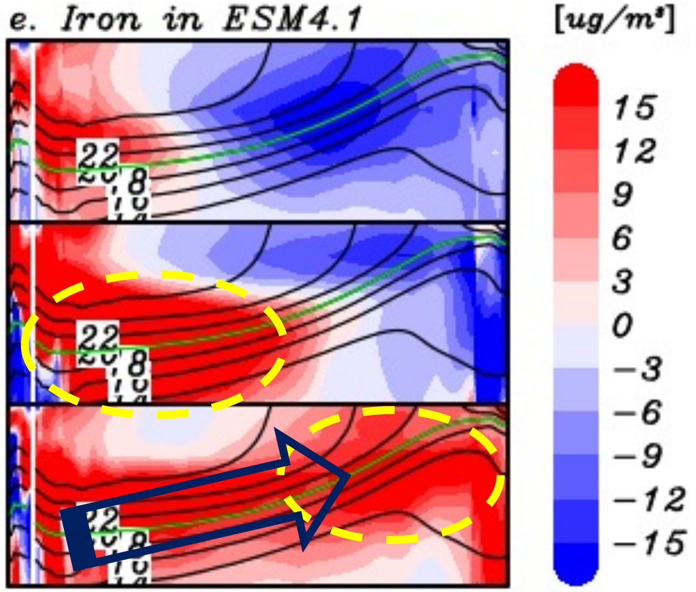

Better capturing ENSO-CHL patterns in ESM4.1

- Negative CHL in WP in mature ENSO
- Positive CHL in EP in decaying ENSO
- WP iron anomalies propagates EP through equatorial undercurrent
- ENSO-related Iron deposition enhances CHL variability

Challenging points

- Spring barrier
- Fire activity

Future work

- ENSO-CHL diversity
- Asymmetric ENSO related CHL, pCO2 rectification on mean fields
- Other climate modes related CHL responses

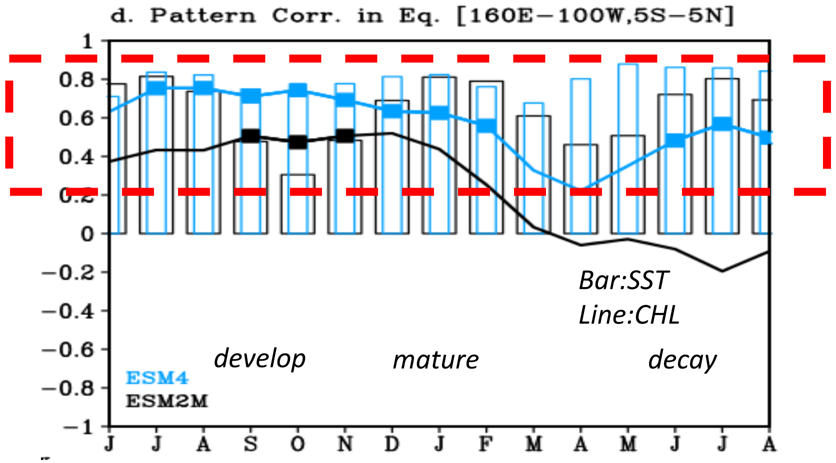

Wildfire-mineral dust coupling: Australia fire -> Blooms in Southern Ocean

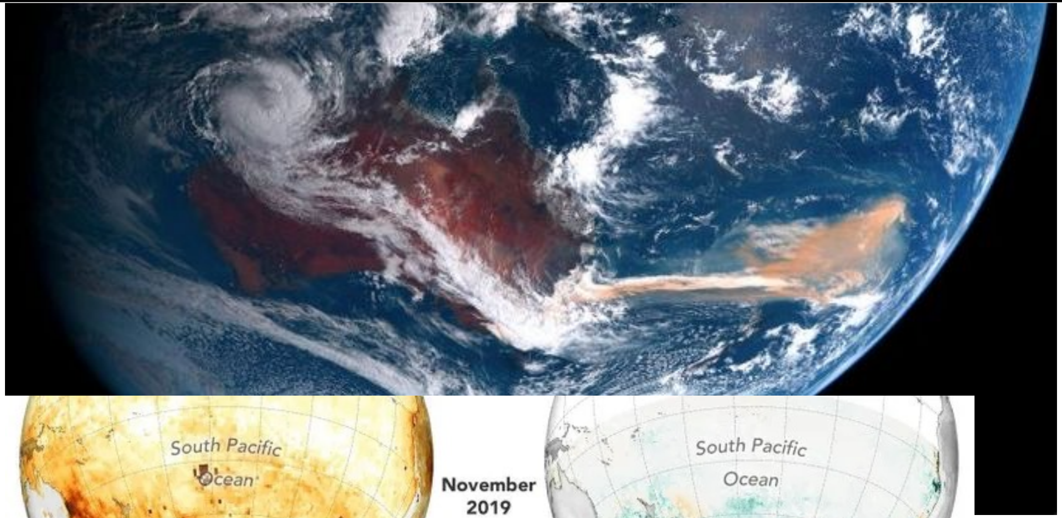

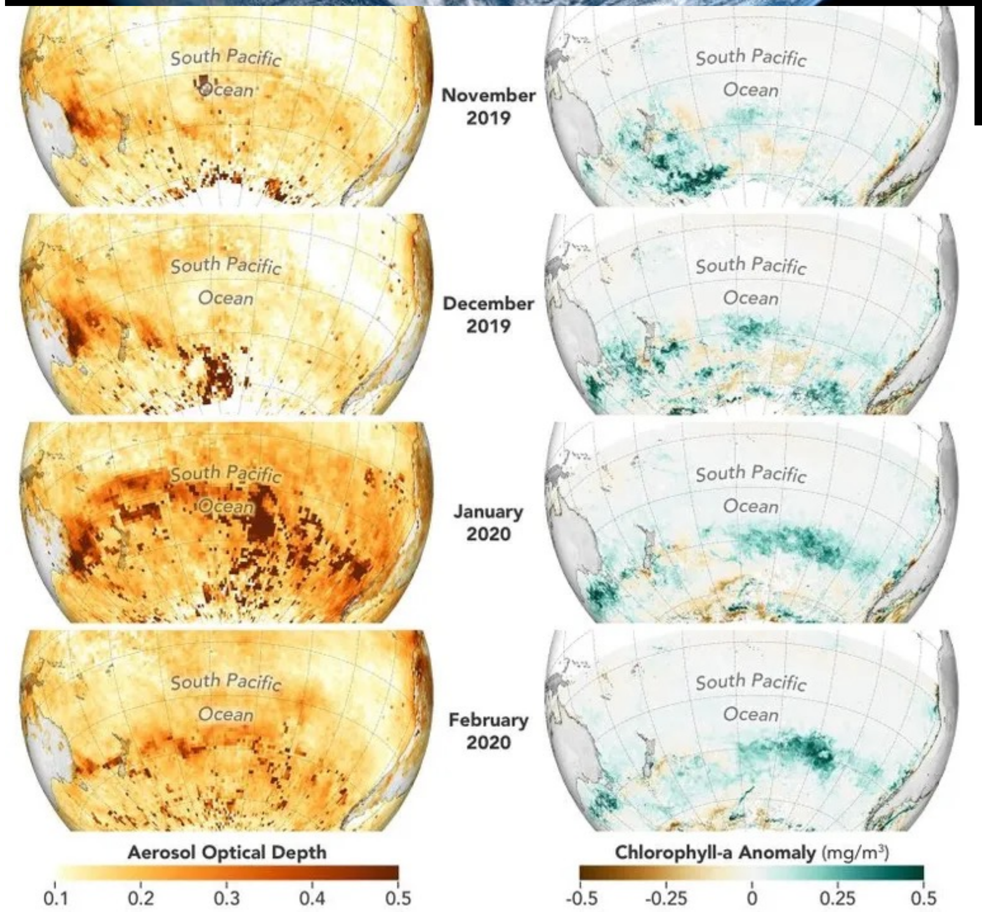

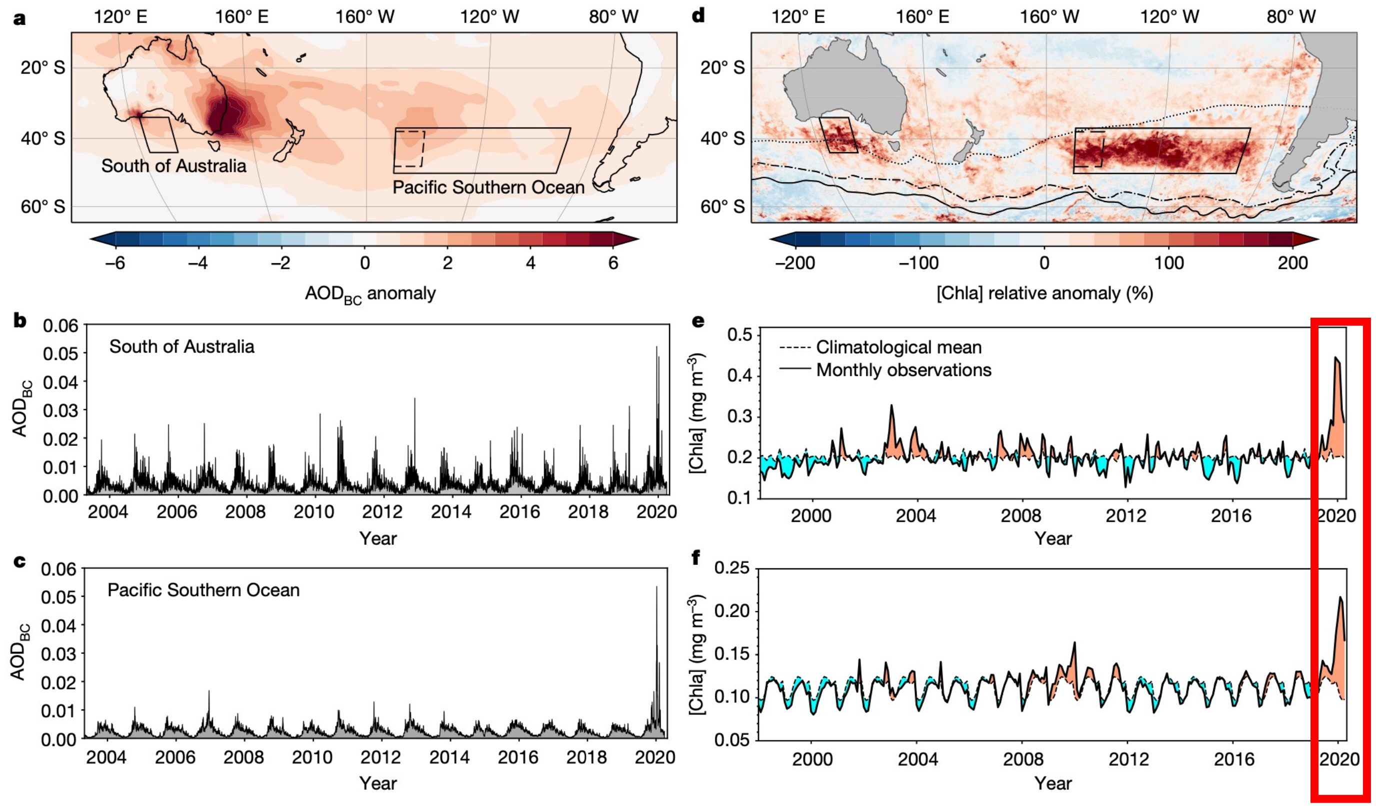

Fig. 1 | Maps of black carbon AOD and [Chla] anomalies and their historical records. a, Cumulative black carbon AOD (AOD_{BC}) anomaly for the 2019–2020 austral summer. **b**, Daily time-series of black carbon AOD for waters south of Australia (solid black box in panels **a** and **d**). **c**, Daily time-series of black carbon AOD in the Pacific Southern Ocean (solid black box in panels **a** and **d**). **d**, [Chla] relative anomaly for the 2019–2020 austral summer. The dashed box within the 'Pacific Southern Ocean' box is used to show temporal variations of black carbon AOD and [Chla] time-series during the 2019–2020 Australian wildfires in Fig. 2. **e**, Monthly time-series of [Chla] in waters south of Australia (solid black line). Monthly climatological values are shown with a dotted black line. Red and cyan areas denote monthly data higher or lower than climatological values, respectively. **f**, Monthly time-series of [Chla] in the Pacific subantarctic Southern Ocean (south of the Subtropical Front). Dotted, dot-dashed and solid black lines in **d** represent the climatological positions of the Subtropical Front, Subantarctic Front and Polar Front, respectively[48].

Tang et al 2021 Nature

Nitrogen loaded by River runoff & Nitrogen depositions in the Arctic Ocean

Human-induced N fertilization in Arctic Ocean

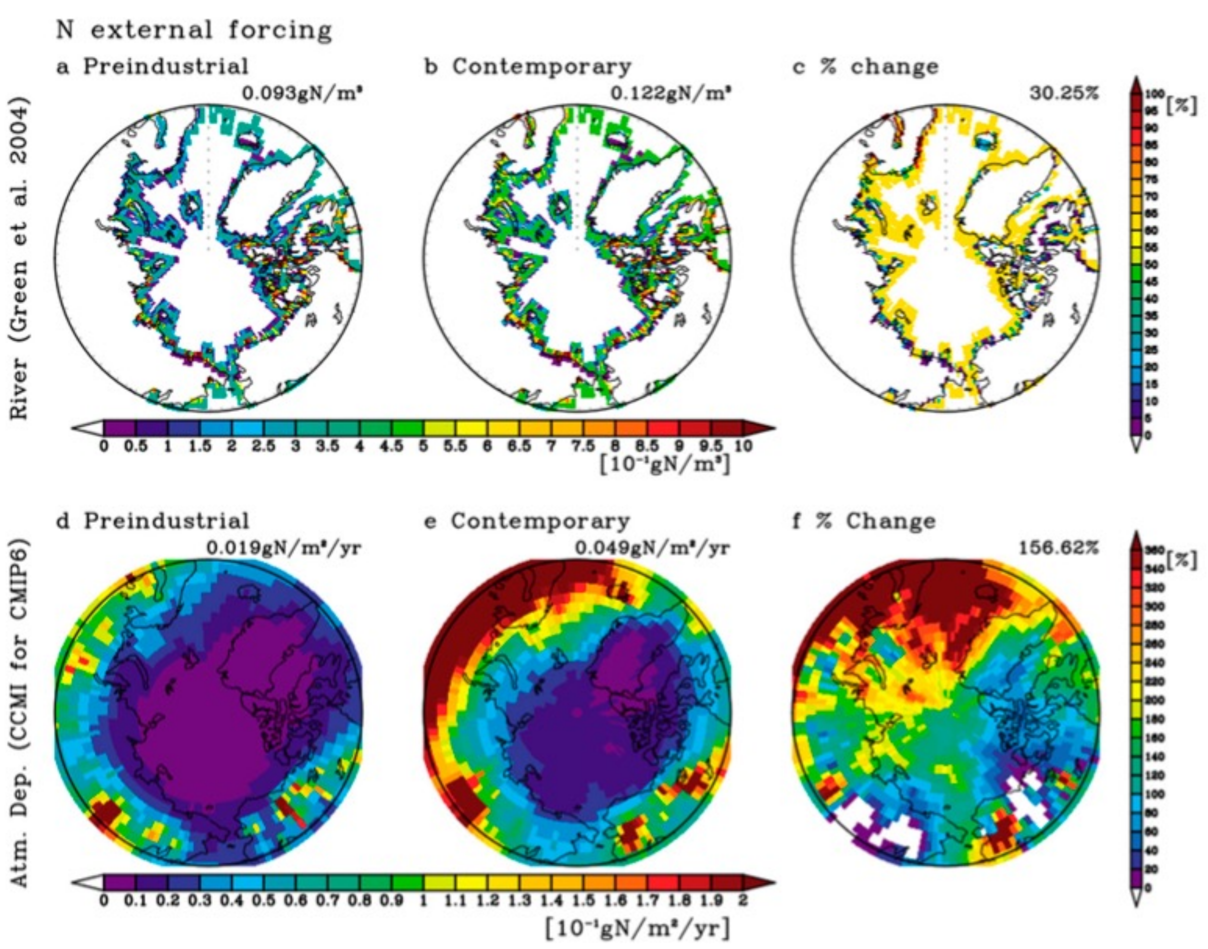

FIG. 1. External forcing N used in present study: (left) preindustrial, (center) contemporary, and (right) percentage change between preindustrial and contemporary amounts through (top) river and (bottom) atmospheric depositions and their quantities averaged for the pan-Arctic (top-right value in each panel).

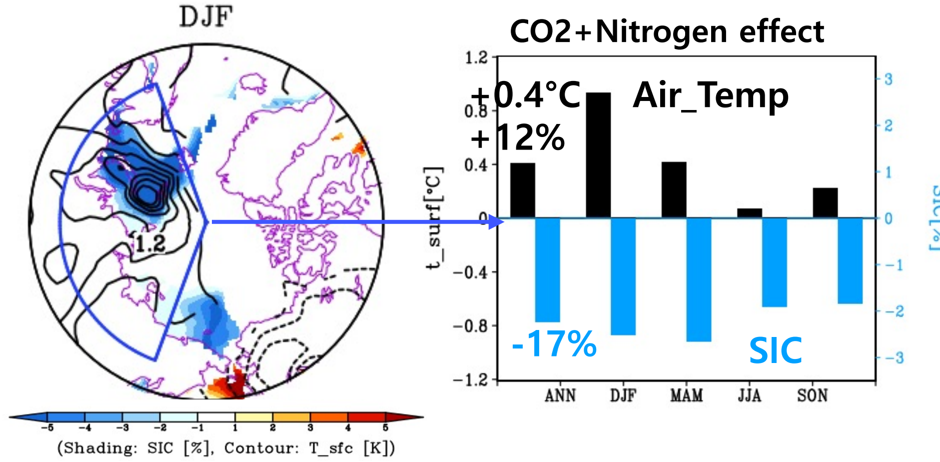

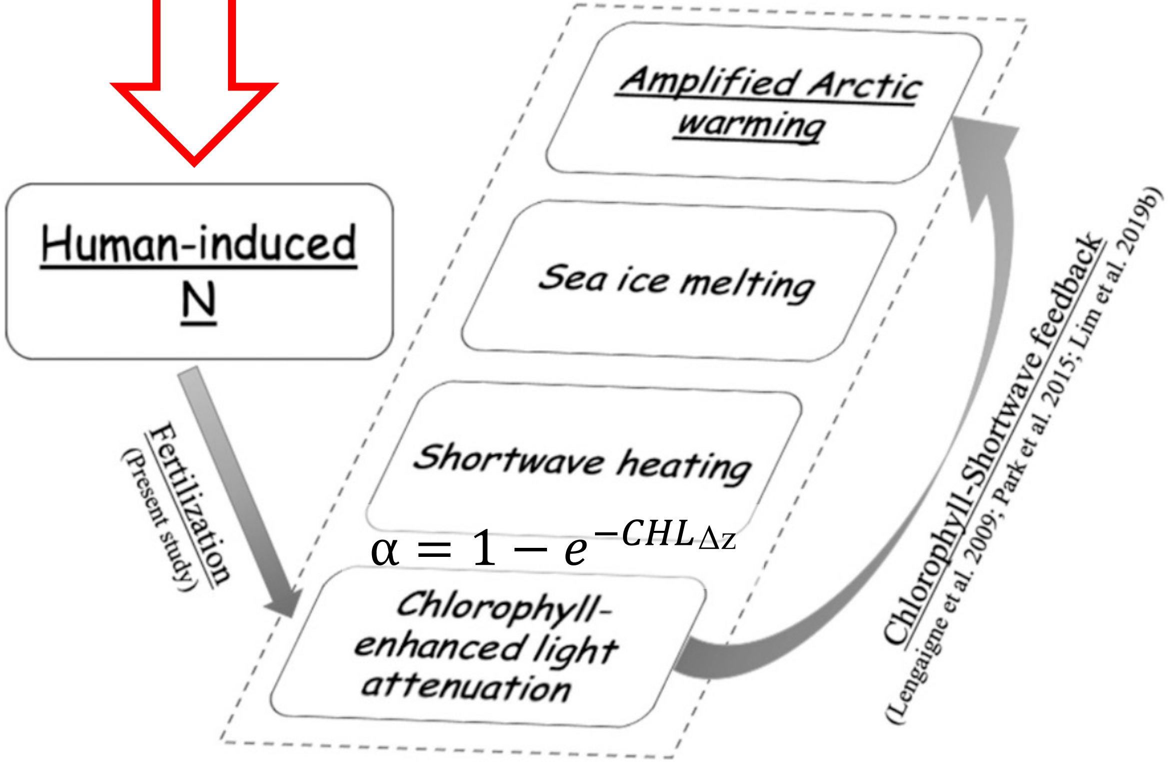

" Arctic warming amplified by Human-induced N "

Lim et al. 2021 JC

Iron export from terrestrial sediment

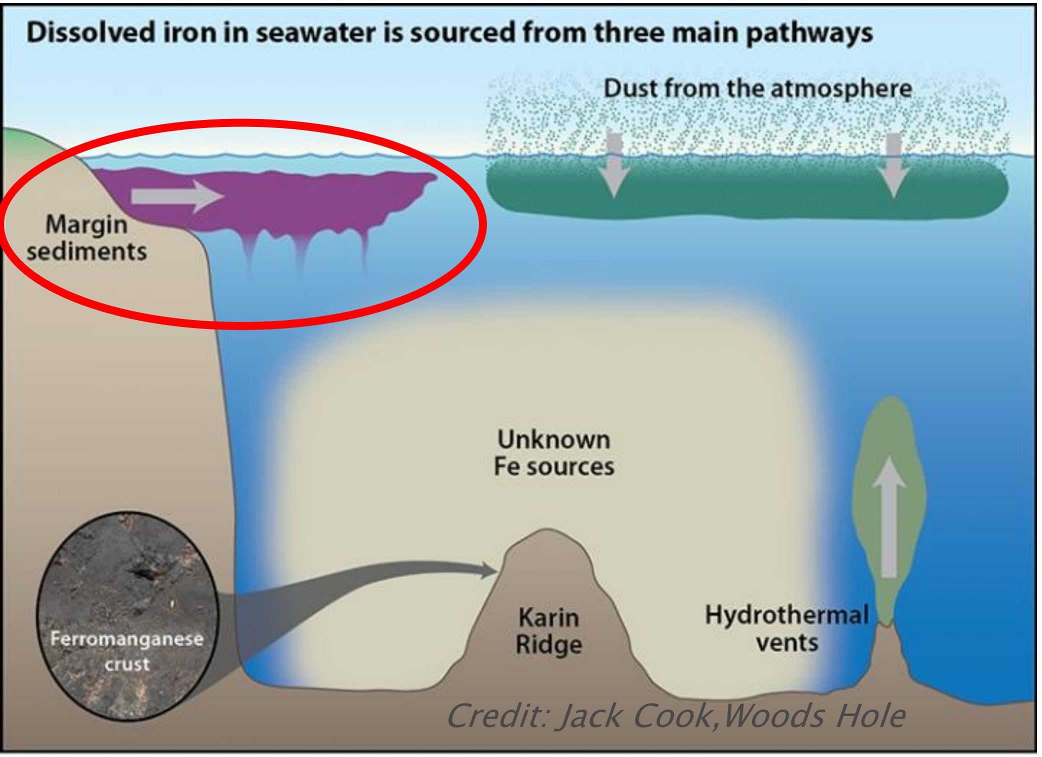

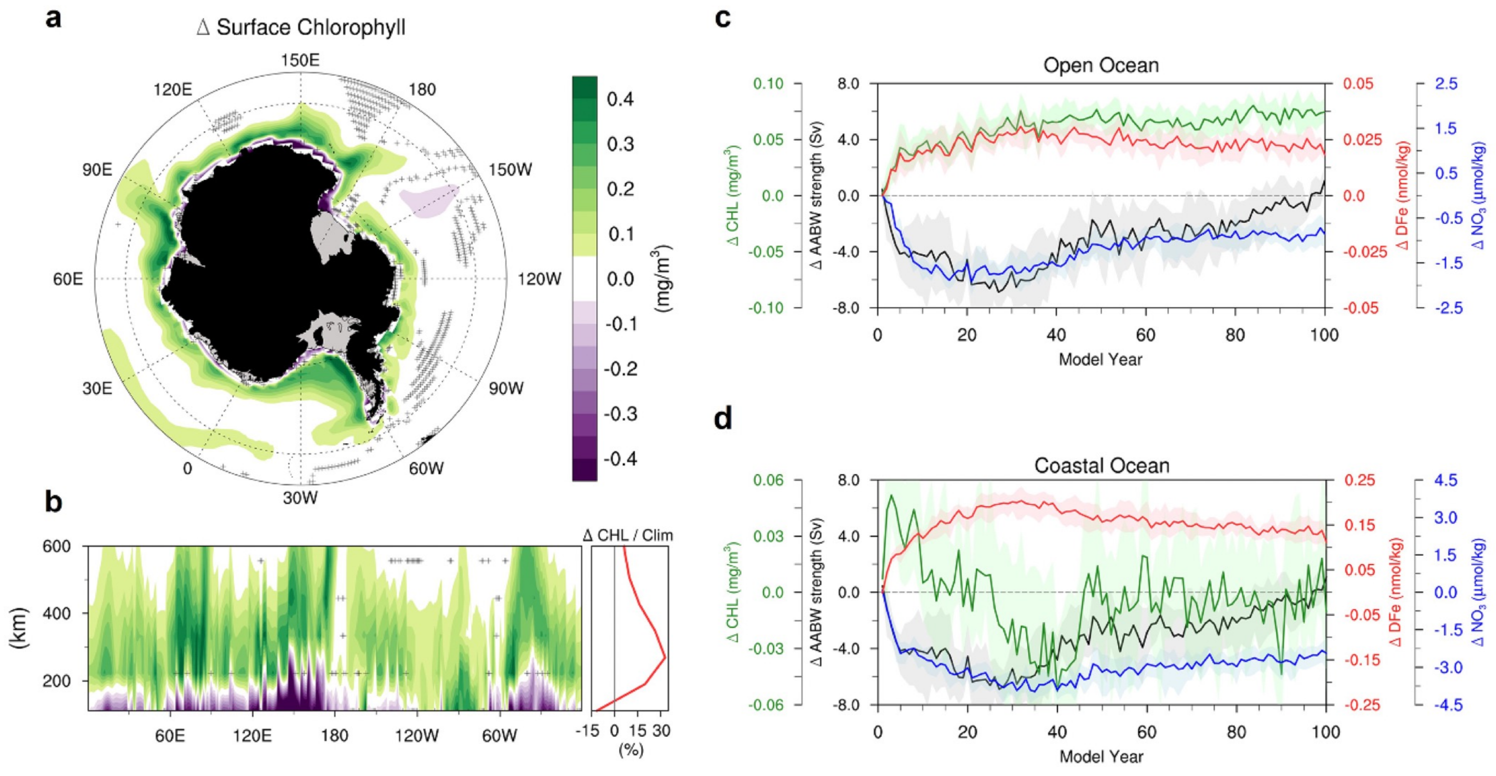

Meltwater driven stratification -> less upwelling of subsurface nitrate

Increased river runoff -> more terrestrial sediment iron source in Antarctic coastal environment

Oh et al. 2022 ERL

Atmospheric circulation driven ice and chlorophyll variabilities

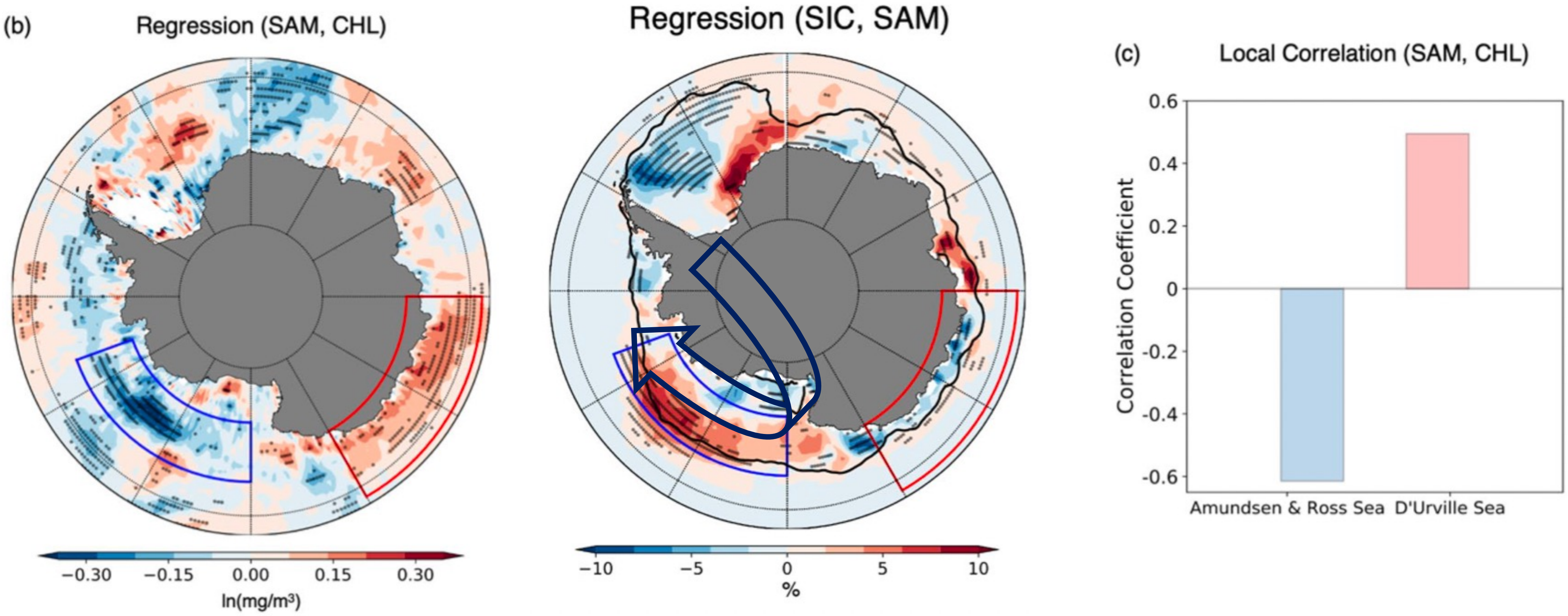

western Amundsen–Ross Sea low pressure -> Sea ice export -> light reflection

Noh et al. 2022 Scientific reports

Prediction of Marine heatwave driven ecosystem vulnerability

Successful Prediction of Marine Heatwaves → MHWs-Satellite Ocean color extremes

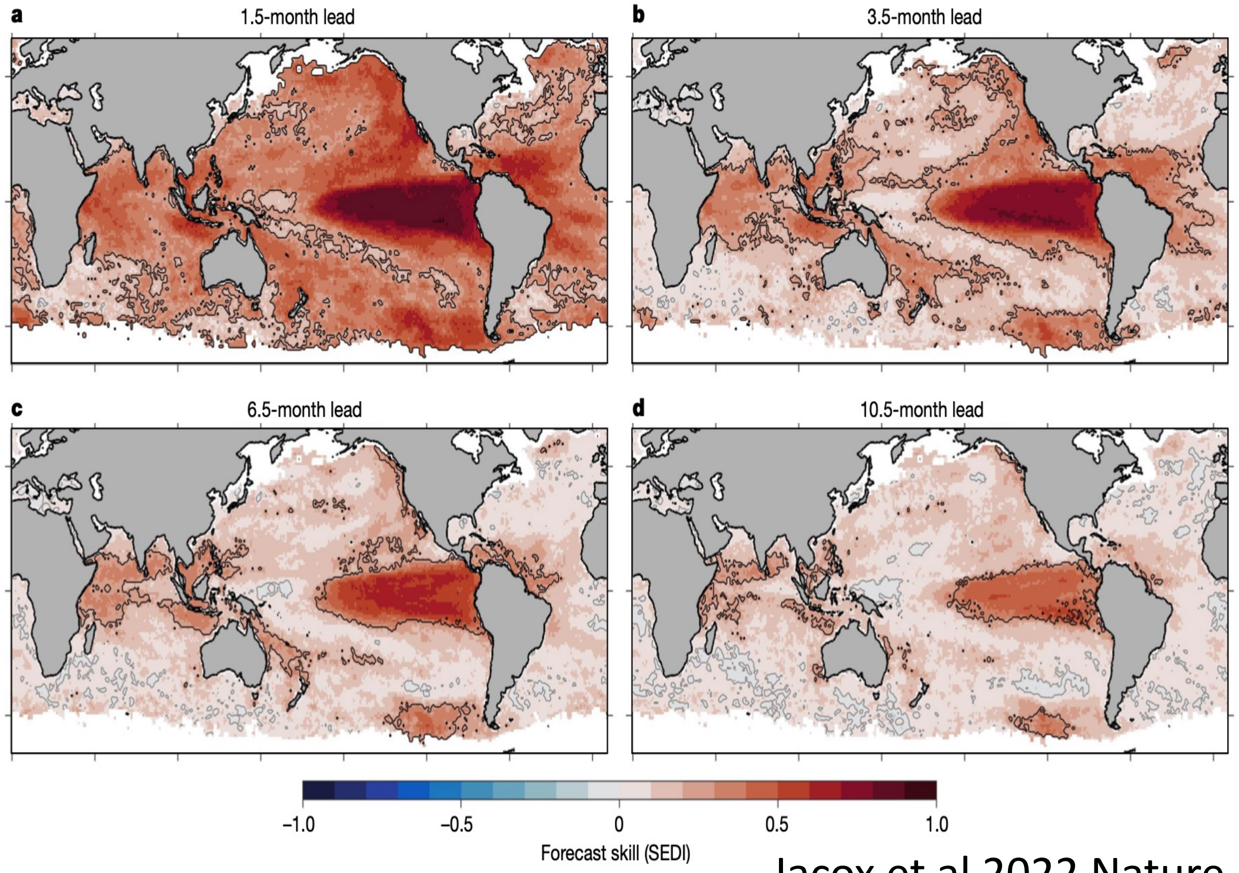

Jacox et al 2022 Nature

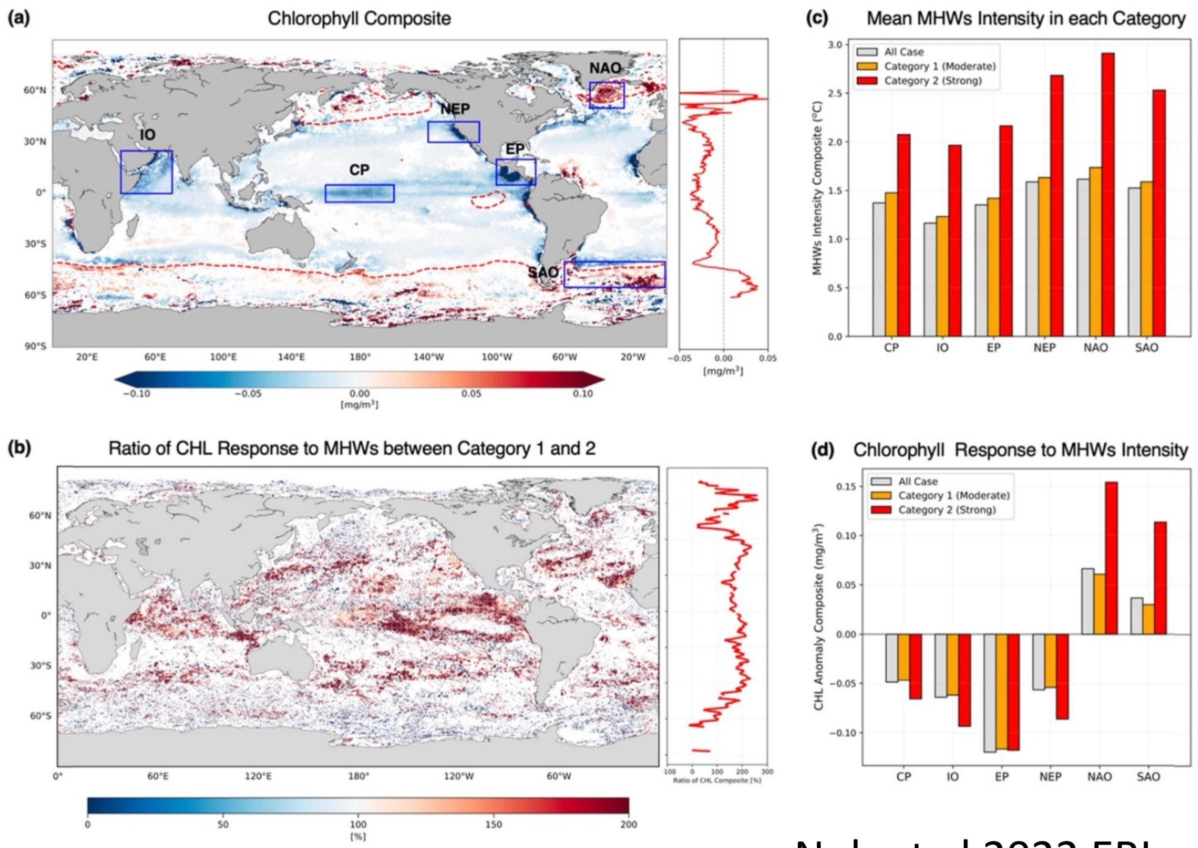

Noh et al 2022 ERL

*Forecasting system for marine heatwaves-driven ecosystem extremes to provide fisheries managements

Conclusion

Comprehensive coupling processes **“physical ocean circulation – Biogeochemistry – Land – Atmosphere”** should be considered in the Earth System Model.

- **Current Climate Extreme:** Physical and Biogeochemical dynamics
- **Changing Climate:** Aerosol, dust, meltwater, sediment, ocean current transport of nutrient

➢ **Increasing chances of predictability** in the model to support decision making for policy makers for long term **marine ecosystem resilience** and **fisheries managements**

Hyung-Gyu Lim (hyl021@ucsd.edu)